Electronic Supplementary Material (ESI) for Chemical Science.

Visualizing Changes in Mitochondrial Mg^{2+} During Apoptosis with Organelle-Targeted Triazole-Based Ratiometric Fluorescent Sensors

Guangqian Zhang, Jessica J. Gruskos, Mohammad S. Afzal, and Daniela Buccella*

Department of Chemistry, New York University, New York, New York 10003

e-mail: dbuccella@nyu.edu

Contents **Page No.**

1. Supplemental figures S2
1.1. Magnesium-binding properties of new sensors S2
1.2. Metal selectivity profiles S4
1.3. Calcium-binding properties of new sensors S5
1.4. pH Dependence of fluorescence response S6
1.5. Fluorescence imaging of Mg^{2+} response and co-localization analysis S7
1.6. Fluorescence imaging of apoptotic HeLa cells S8
1.7. Fluorescence imaging of Mg^{2+} in apoptotic HeLa cells treated with TPA S9
2. Synthetic procedures S10
2.1. Synthesis of alkyne precursor 5-AM S10
2.2. Syntheses of azides S12
2.3. Assembly of triazole-containing sensors S15
3. Spectroscopic methods S17
4. Cell culture and imaging protocols S19
5. NMR spectroscopy data for new sensors S21
6. HPLC data for new sensors S32
7. References S41

1. Supplemental Figures

1.1. Magnesium-binding properties of new sensors

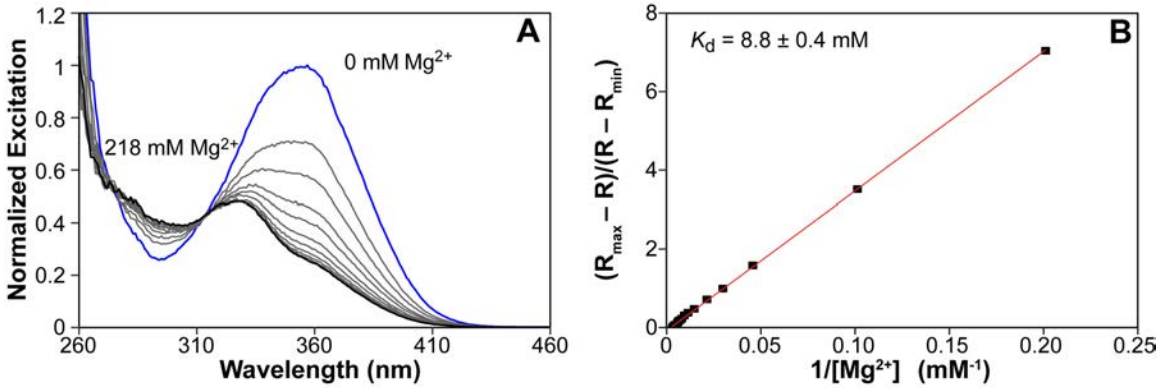

Figure S1. (A) Representative fluorescence excitation spectrum of a 2 μM solution of compound **7a** in aqueous buffer at pH 7.0, 25 °C, as a function of magnesium concentration. Emission wavelength: 483 nm. (B) Representative double reciprocal plot for the change in fluorescence ratio as a function of magnesium concentration. Excitation wavelengths: λ_1= 328 nm, λ_2= 354 nm. Dissociation constant corresponds to the average of three independent titrations.

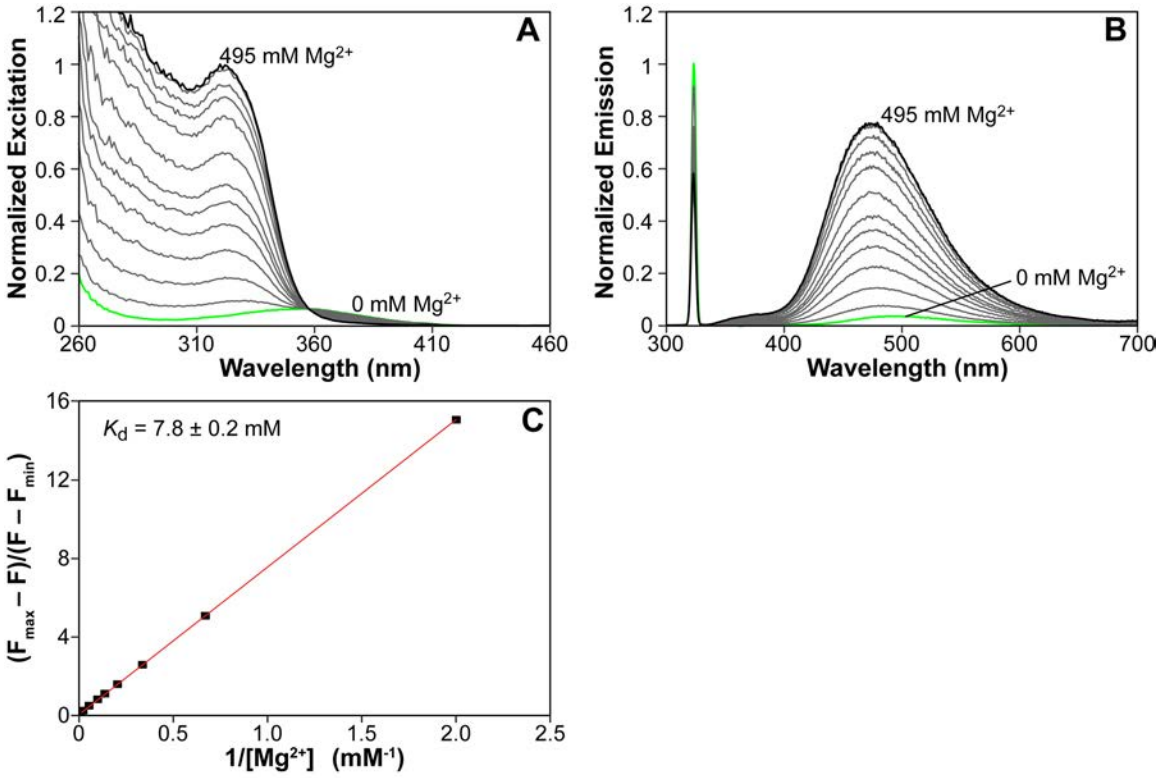

Figure S2. (A) Representative fluorescence excitation spectrum of a 5 μM solution of compound **7b** in aqueous buffer at pH 7.0, 25 °C, as a function of magnesium concentration. Emission wavelength: 474 nm. (B) Fluorescence emission spectrum. (C) Representative double reciprocal plot for the change in fluorescence emission as a function of magnesium concentration. Excitation wavelength: 323 nm. Dissociation constant corresponds to the average of three independent titrations.

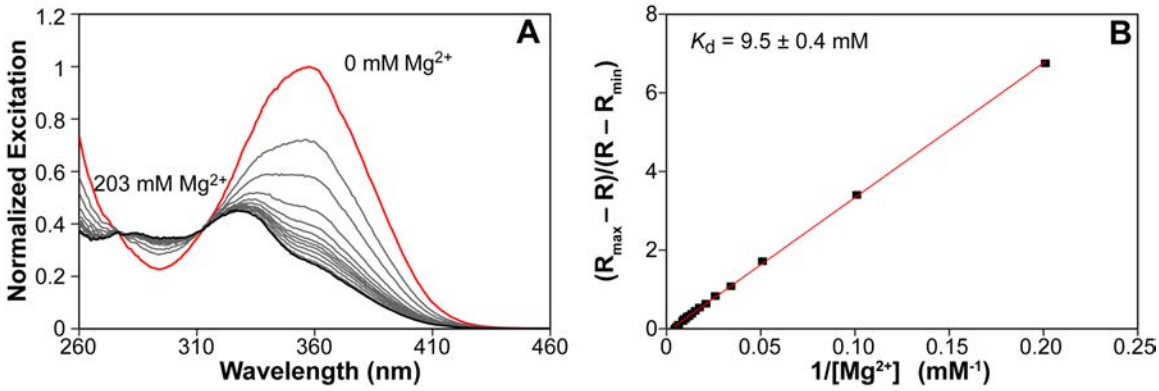

Figure S3. (A) Representative fluorescence excitation spectrum of a 2 μM solution of compound **7c** in aqueous buffer at pH 7.0, 25 °C, as a function of magnesium concentration. Emission wavelength: 482 nm. (B) Representative double reciprocal plot for the change in fluorescence ratio as a function of magnesium concentration. Excitation wavelengths: λ_1= 330 nm, λ_2= 356 nm. Dissociation constant corresponds to the average of three independent titrations.

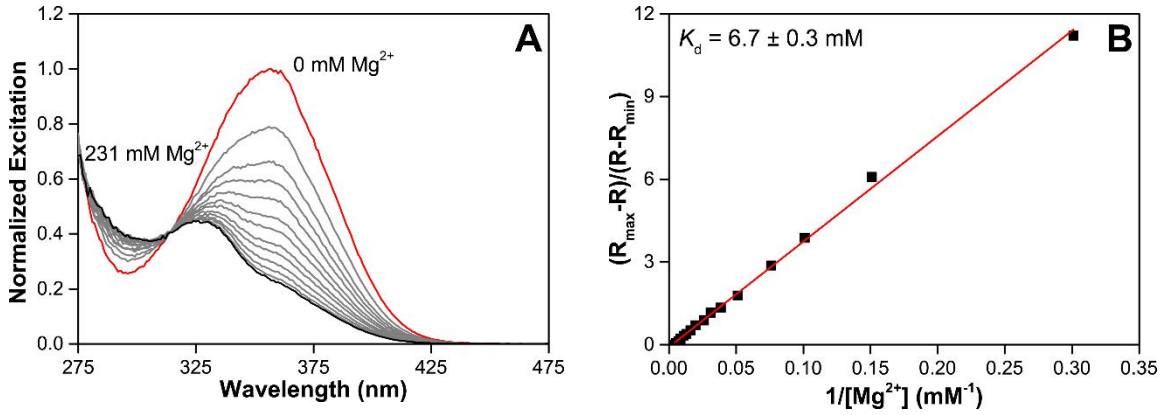

Figure S4. (A) Representative fluorescence excitation spectrum of a 2 μM solution of **Mag-*mito*** in aqueous buffer at pH 7.0, 25 °C, as a function of magnesium concentration. Emission wavelength: 482 nm. (B) Representative double reciprocal plot for the change in fluorescence ratio as a function of magnesium concentration. Excitation wavelengths: λ_1= 330 nm, λ_2= 356 nm. Dissociation constant corresponds to the average of three independent titrations.

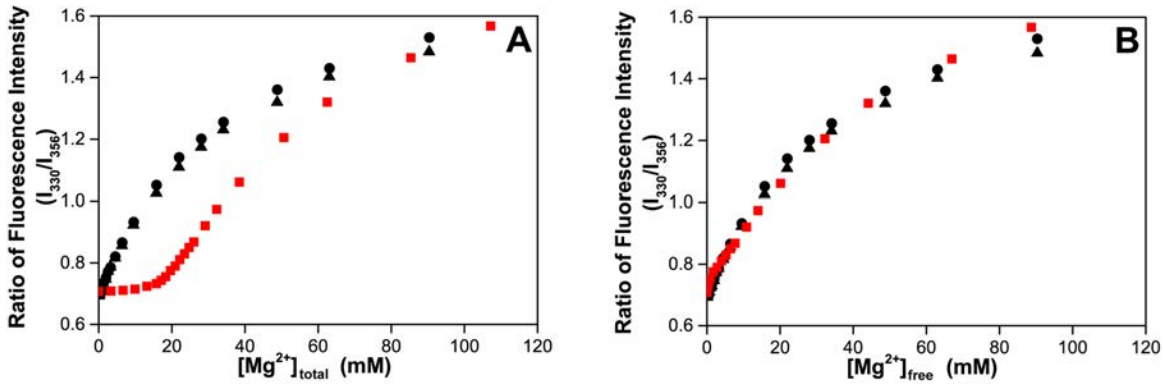

Figure S5. Representative titration curves of a 2 µM solution of compound **7c** in aqueous buffer at pH 7.0, 25 °C, as a function of total (A) and free (B) magnesium concentration. Red squares: titration conducted in the presence of ATP (18.4 mM). Black circles and triangles: titrations conducted without ATP. The free magnesium concentration in titrations conducted with ATP was calculated from the total magnesium concentration considering simple dissociation of MgATP complex (K_d MgATP= 50 µM).[1]

1.2. Metal selectivity profiles

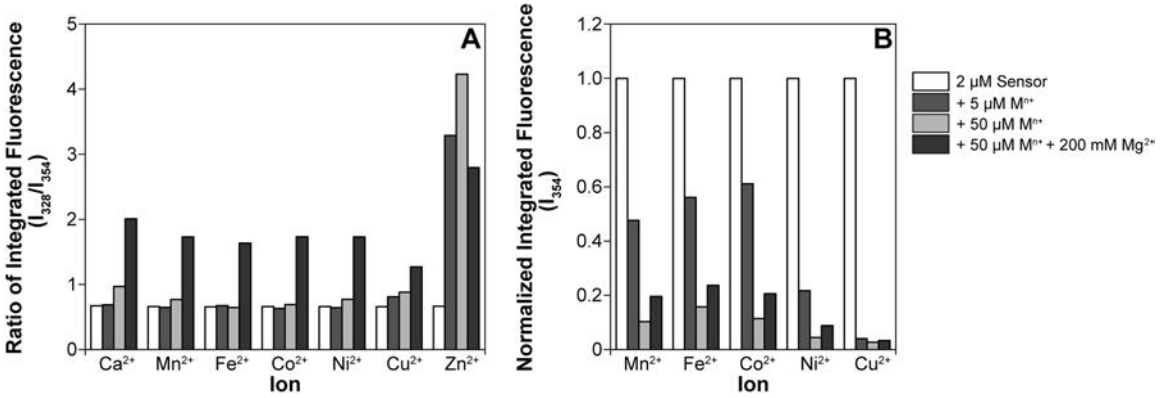

Figure S6. Metal selectivity plots for compound **7a** in aqueous buffer at pH 7.0. (A) Ratio of integrated fluorescence emission ($I\lambda_1/I\lambda_2$), excitation wavelengths: λ_1= 328 nm, λ_2= 354 nm. (B) Integrated fluorescence emission ($I\lambda_2$), excitation wavelength: 354 nm.

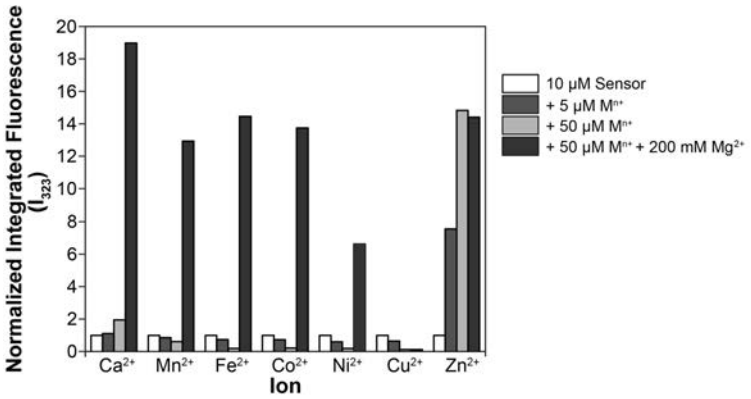

Figure S7. Metal selectivity plot for compound **7b** in aqueous buffer at pH 7.0. Excitation wavelength: 323 nm.

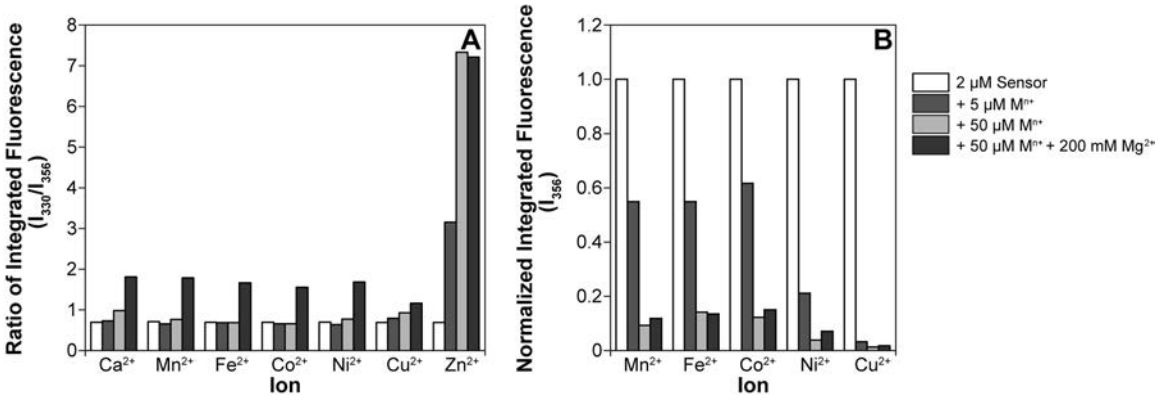

Figure S8. Metal selectivity plots for compound **7c** in aqueous buffer at pH 7.0. (A) Ratio of integrated fluorescence emission ($I\lambda_1/I\lambda_2$), excitation wavelengths: λ_1= 330 nm, λ_2= 356 nm. (B) Integrated fluorescence emission ($I\lambda_2$), excitation wavelength: 356 nm.

1.3. Calcium-binding properties of new sensors

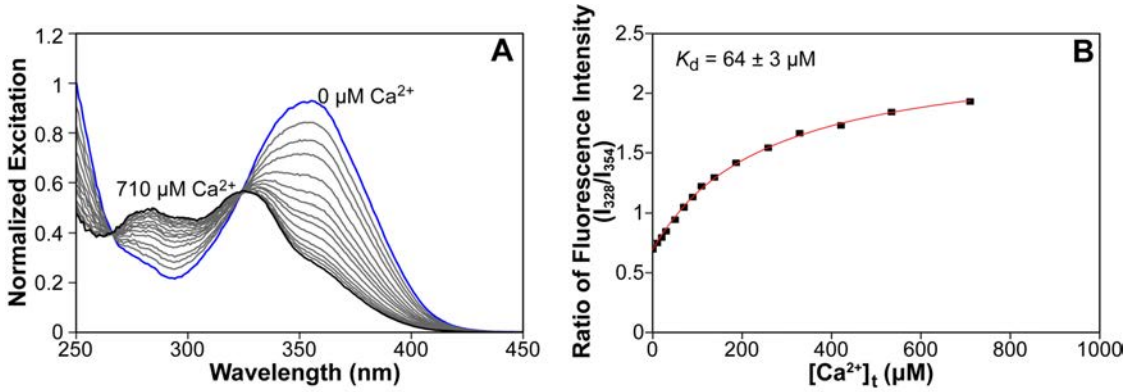

Figure S9. (A) Representative fluorescence excitation spectrum of a 2 μM solution of compound **7a** in aqueous buffer at pH 7.0, 25 °C, as a function of calcium concentration. Emission wavelength: 483 nm. (B) Representative binding isotherm. Reported dissociation constant is the average of three independent titrations.

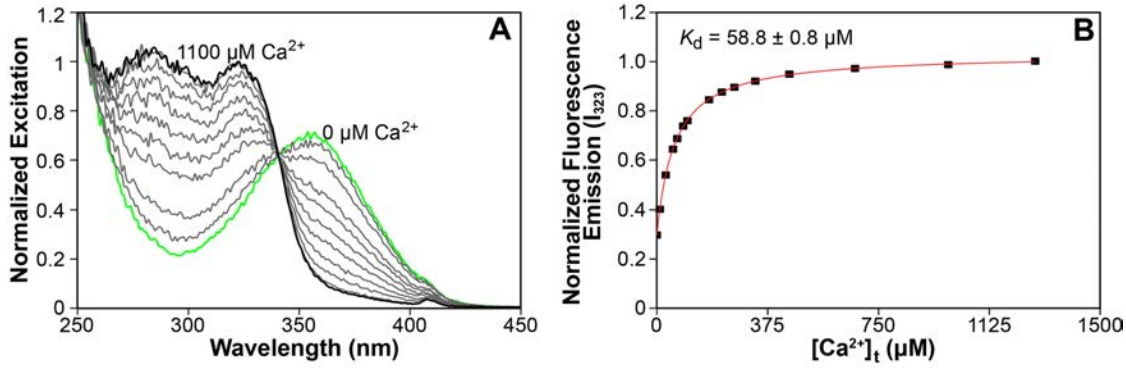

Figure S10. (A) Representative fluorescence excitation spectrum of a 5 μM solution of compound **7b** in aqueous buffer at pH 7.0, 25 °C, as a function of calcium concentration. Emission wavelength: 474 nm. (B) Representative binding isotherm. Reported dissociation constant is the average of three independent titrations.

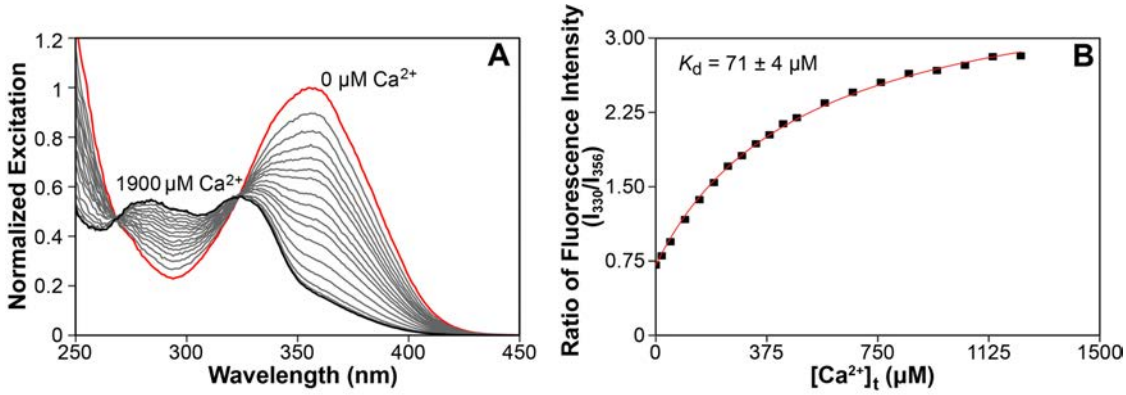

Figure S11. (A) Representative fluorescence excitation spectrum of a 2 μM solution of compound **7c** in aqueous buffer at pH 7.0, 25 °C, as a function of calcium concentration. Emission wavelength: 482 nm. (B) Representative binding isotherm. Reported dissociation constant is the average of three independent titrations.

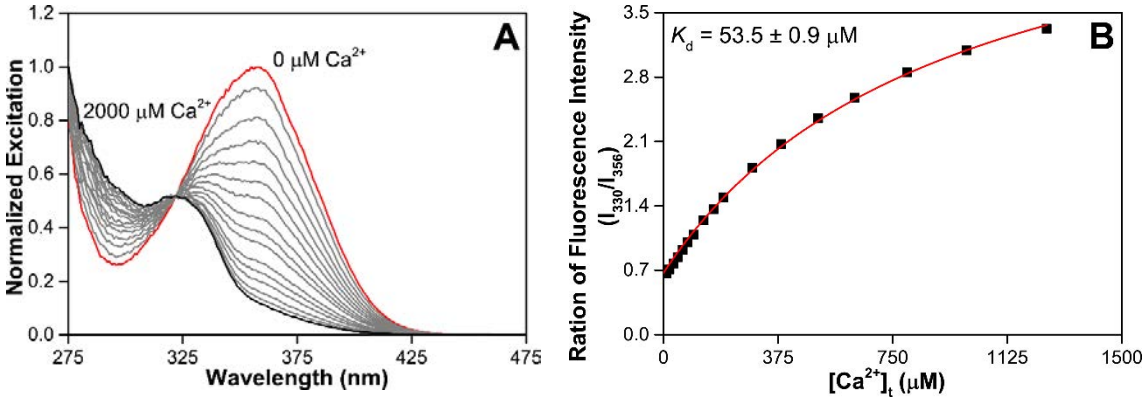

Figure S12. (A) Representative fluorescence excitation spectrum of a 2 μM solution of **Mag-*mito*** in aqueous buffer at pH 7.0, 25 °C, as a function of calcium concentration. Emission wavelength: 482 nm. (B) Representative binding isotherm. Reported dissociation constant is the average of three independent titrations.

1.4. pH Dependence of fluorescence response

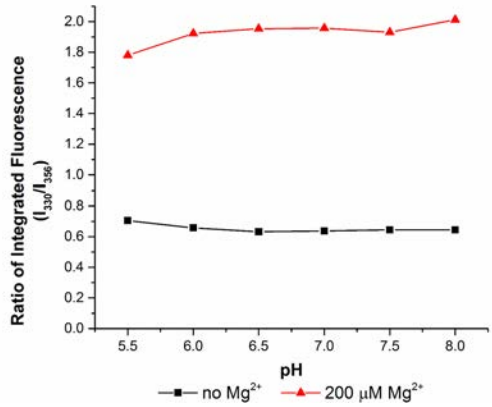

Figure S13. Fluorescence ratio ($I\lambda_1/I\lambda_2$) of a 1 μM solution of **7c** in aqueous buffer as a function of pH (50 mM buffer, 100 mM KCl, 25 °C). Excitation wavelengths: λ_1= 330 nm, λ_2= 356 nm.

1.5. Fluorescence imaging of Mg^{2+} response and co-localization analysis

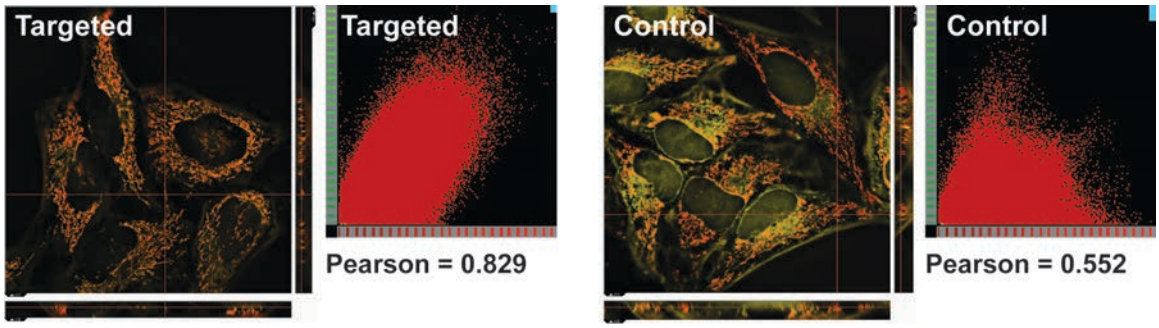

Figure S14. Image overlay and 2-D histograms showing the co-localization of **Mag-*mito*** (left) and untargeted control (**7c**, right) with MitoTracker green FM in live HeLa cells. Magnesium dyes are pseudo-colored in yellow, whereas mitochondrial stain is pseudo-colored in red. The analysis was conducted over the cell volume, reconstructed from a z-stacked series of images.

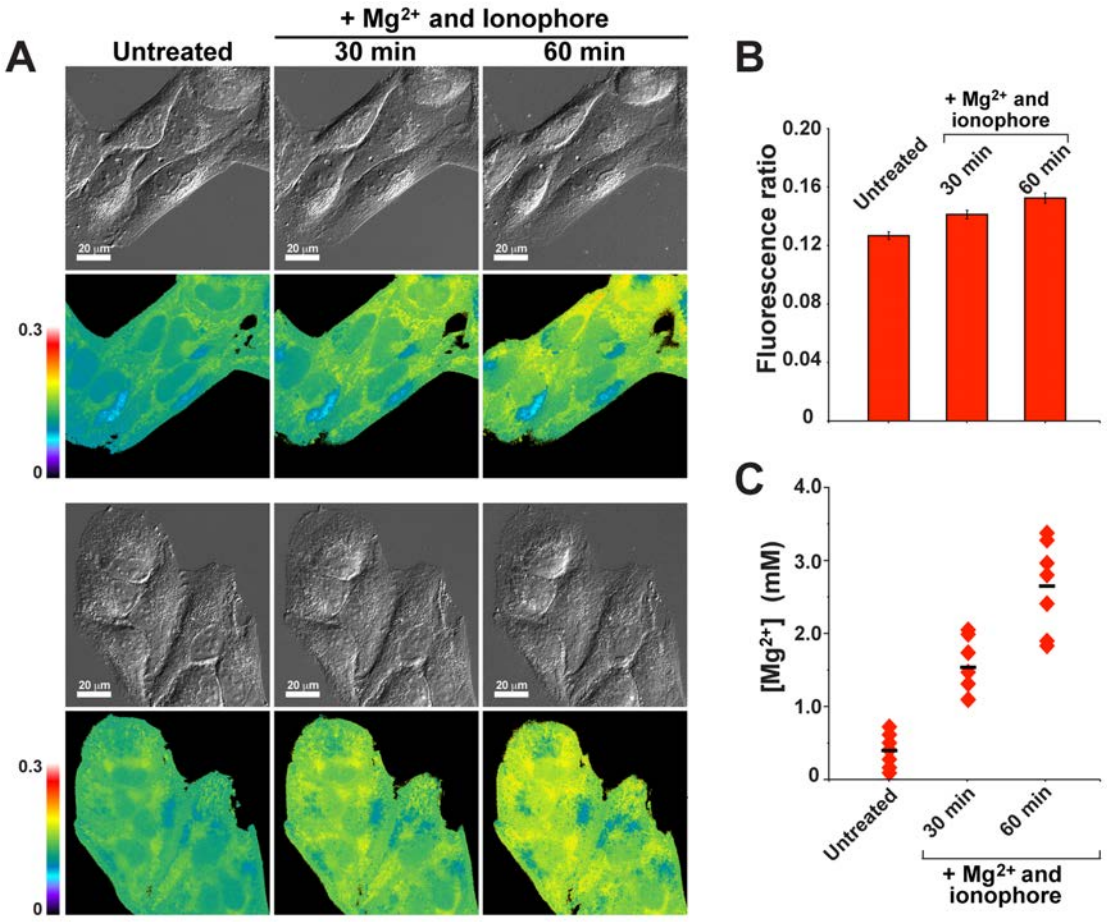

Figure S15. (A) Fluorescence microscopy images of live HeLa cells treated with 1 μM of compound **7c-AM**, before and after treatment with 2.5 μM magnesium ionophore 4-bromo-A-23187 and 20 mM exogenous $MgCl_2$. For each set of images (top) DIC images; (bottom) fluorescence ratio images. (B) Average fluorescence ratio per cell before and after treatment with exogenous magnesium and ionophore. Error bars = standard deviation of the mean, *N* = 9. (C) Average free magnesium concentration per cell determined from calibration of the fluorescence ratio.

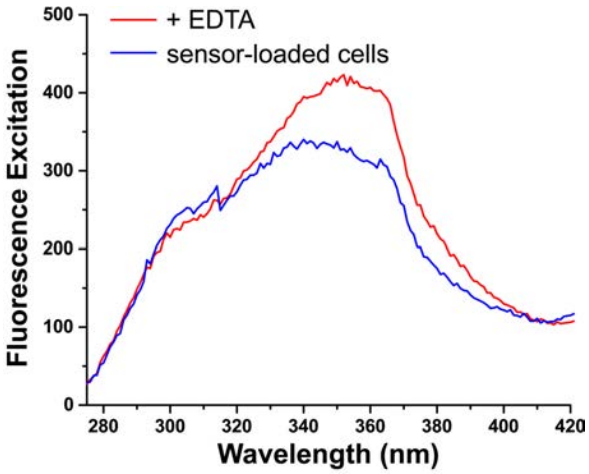

Figure S16. Fluorescence excitation spectrum of HeLa cells treated with 6 μM **7c-AM** suspended in HBSS. Blue trace: sensor-loaded cells, red trace: sensor-loaded cells treated with 50 mM EDTA and 2.5 μM magnesium ionophore 4-bromo-A-23187. λ_{EM} = 482 nm.

1.6. Fluorescence imaging of apoptotic HeLa cells

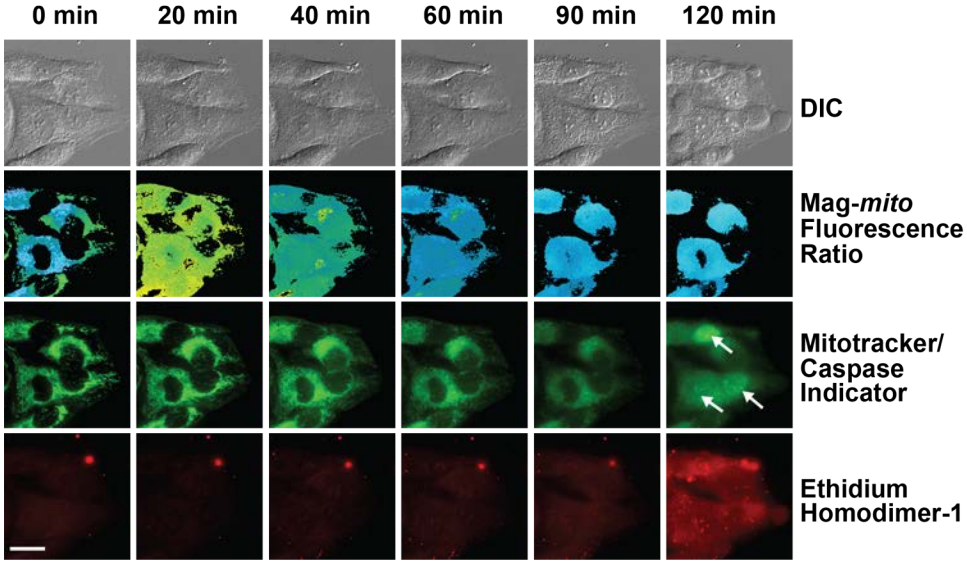

Figure S17. Selected images of a representative time-course apoptosis experiment monitoring Staurosporine-treated HeLa cells stained with 1 μM **Mag-*mito*-AM**. From top to bottom: DIC; fluorescence ratio obtained with **Mag-*mito***; MitoTracker and CellEvent Caspase 3/7 channel; Ethidium homodimer-1 channel. Signal of the magnesium sensor and the MitoTracker becomes diffuse after ~40 min, likely due to mitochondrial membrane depolarization and dye leakage. Caspase activation is apparent between 90-120 min (arrows). Scale bar= 20 μm.

1.7. Fluorescence imaging of Mg^{2+} in apoptotic HeLa cells treated with TPA

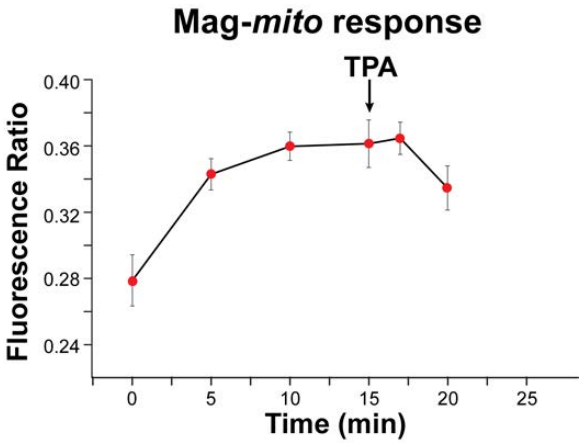

Figure S18. Changes in fluorescence ratio over time in Staurosporine-treated HeLa cells stained with 1 μM **Mag-*mito*-AM**. An aliquot of 10 μM of tris-(2-pyridylmethyl)amine (TPA), a rapid Zn^{2+} chelator with picomolar affinity, was added 15 min after induction of apoptosis to trap any zinc. (Note: signal from mitotracker green and the fluorescent Mg^{2+} sensor becomes diffuse, and organelle structure becomes less defined after 5 min of TPA addition, presumably due to the toxic effects of the chelator on the cells). Error bars: standard deviations.

2. Synthetic Procedures

2-Methoxycarboylmethoxy-*N,N*-bis(methoxycarbonylmethyl)benzene-1,4-diamine,[2] 2,6-diisopropyl-4-methoxyaniline,[3] and 4-iodo-2,6-diisopropylaniline[4] were prepared according to literature procedures. All other reagents were purchased from commercial sources and used as received. Solvents were purified and degassed by standard procedures. NMR spectra were acquired on Bruker Avance 400 spectrometers. ^{1}H NMR chemical shifts are reported in ppm relative to $SiMe_4$ (δ = 0) and were referenced internally with respect to residual protio impurity in the solvent (δ = 7.26 for $CHCl_3$, 2.50 for DMSO-d_5, 5.32 for $CHDCl_2$, 3.31 for CHD_2OD, 1.94 for CHD_2CN). ^{13}C NMR chemical shifts are reported in ppm relative to $SiMe_4$ (δ = 0) and were referenced internally with respect to the solvent signal (δ 77.16 for $CDCl_3$, 39.52 for DMSO-d_6, 53.84 for CD_2Cl_2, 49.00 for CD_3OD, 1.32 for CD_3CN). ^{31}P NMR chemical shifts are reported in ppm relative to H_3PO_4 (δ = 0) and were referenced externally against a H_3PO_4 standard. Coupling constants are reported in Hz. Infrared spectra were acquired on a Thermo Scientific Nicolet 6700 FT-IR Spectrometer. Melting points were collected on a BUCHI 510 melting point apparatus and are reported uncorrected. Low-resolution mass spectra were acquired on an Agilent 1100 series LC/MSD trap spectrometer, using electrospray (ES) ionization. High-resolution mass spectrometry (HRMS) analyses were conducted on an Agilent 6224 TOF LC/MS Mass Spectrometer using ES ionization. Analytical thin layer chromatography (TLC) was performed on SorbTech polyester-backed 200 µm silica gel sheets. Preparative TLC was performed on SorbTech 1000 µm silica gel plates. Reversed-phase HPLC analyses were conducted on an Agilent 1260 system with UV-Vis absorption and fluorescence detection, using a Poroshell C18 reversed phase column (4.6×50 mm, 2.7 µm particle size) and eluting with a gradient of 10% to 100% acetonitrile/water (+ 0.1% trifluoroactic acid) over 7 min.

2.1. Synthesis of Alkyne precursor, 5-AM

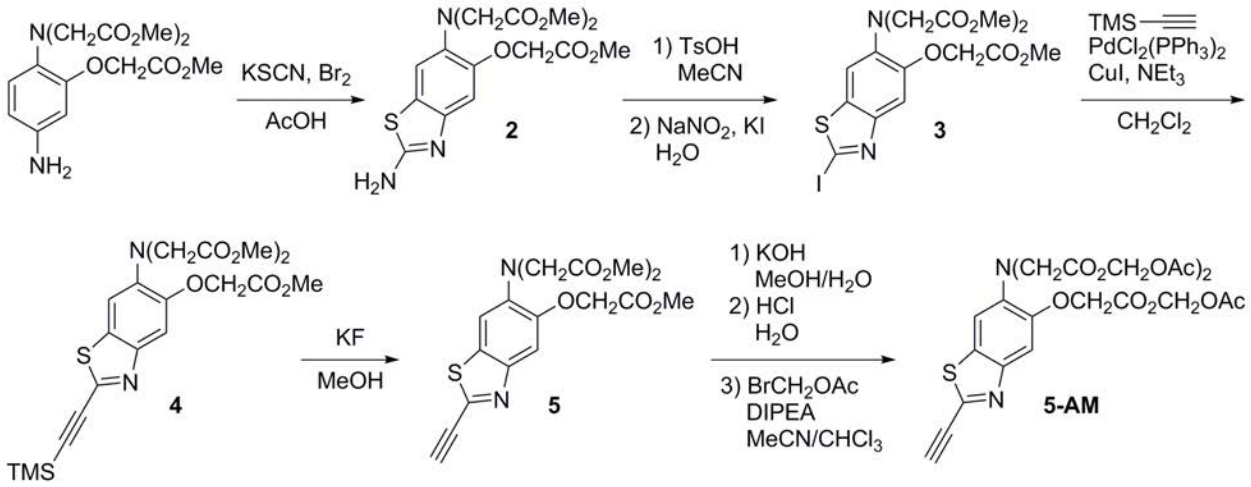

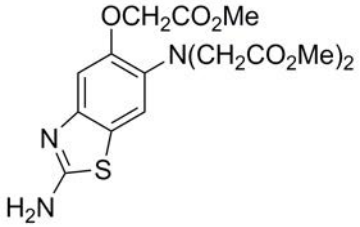

Synthesis of dimethyl 2,2'-((2-amino-5-(2-methoxy-2-oxoethoxy)benzo[*d*]thiazol-6-yl)azanediyl)diacetate (2)

A solution of 2-Methoxycarboylmethoxy-*N,N*-bis(methoxycarbonyl-methyl)benzene-1,4-diamine (11.80 g, 34.69 mmol) and potassium thiocyanate (13.48 g, 138.69 mmol) in acetic acid (120 mL) was stirred at room temperature for 1 h and then cooled to 0 °C. The resulting suspension was treated with a solution of bromine (6.09 g, 38.14 mmol) in acetic acid (30 mL) added dropwise at 0 °C. The mixture was warmed to room temperature and allowed to stir for 60 h, after which it was poured onto water (1 L) and the precipitate was collected by filtration. The solid was suspended in dilute aqueous NH_4OH (500 mL) and re-collected by filtration. The solid was dissolved in hot EtOAc (500 mL) and the hot solution was filtered through a pad of silica gel. The filtrate was concentrated to 50 mL and cooled to room temperature. The precipitate was collected by filtration, washed with cold EtOAc, and dried under vacuum to afford product **2** as a pale yellow powder (9.0 g, 65%, R_f = 0.41 in EtOAc). M.p. 164-165 °C. ^{1}H NMR (400 MHz, DMSO-d_6, δ): 3.59 (s, 6H), 3.69 (s, 3H), 4.13 (s, 4H), 4.80 (s, 2H), 6.89 (s, 1H), 7.22 (s, 1H), 7.24 (s, 2H). ^{13}C{^{1}H} NMR (100 MHz, DMSO-d_6, δ): 51.3, 51.7, 53.4, 65.6, 104.6, 112.5, 123.6, 133.9, 148.3, 149.0, 166.3, 169.4, 171.2. ESI-MS (m/z): $[M+H]^+$ calcd for $C_{16}H_{19}N_3O_7S$, 398.1; found 398.1.

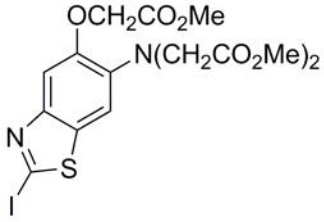

Synthesis of dimethyl 2,2'-((2-iodo-5-(2-methoxy-2-oxoethoxy) benzo[d]thiazol-6-yl)azanediyl)diacetate (3)

A solution of sodium nitrite (138 mg, 2.0 mmol) and potassium iodide (432 mg, 2.6 mmol) in water (1 mL) was added dropwise to a mixture of compound **2** (397 mg, 1.0 mmol) and *p*-toluenesulfonic acid (666 mg, 3.5 mmol) in acetonitrile (4 mL) at 0 °C over 30 min. The reaction mixture was stirred at room temperature overnight. After this period, water (15 mL) was added and the pH was adjusted to 8-9 with addition of solid $NaHCO_3$. The aqueous layer was extracted with EtOAc (3×10 mL) and the combined organics were washed with water (3×15 mL), dried with Na_2SO_4 and concentrated *in vacuo*. The residue was purified by column chromatography on silica gel (2:1 hexanes:EtOAc) to give compound **3** as a white solid (440 mg, 87%, R_f = 0.62 in 1:1 hexanes:EtOAc). M.p. 128-129 °C. ^{1}H NMR (400 MHz, $CDCl_3$, δ): 3.74 (s, 6H), 3.79 (s, 3H), 4.26 (s, 4H), 4.72 (s, 2H), 7.33 (s, 1H), 7.39 (s, 1H). ^{13}C{^{1}H} NMR (100 MHz, $CDCl_3$, δ): 52.1, 52.4, 53.9, 66.0, 103.0, 106.5, 110.5, 133.3, 139.2, 150.0, 150.1, 168.8, 171.5. ESI-MS (m/z): $[M+Na]^+$ calcd for $C_{16}H_{17}IN_2O_7S$, 531.0; found 531.0.

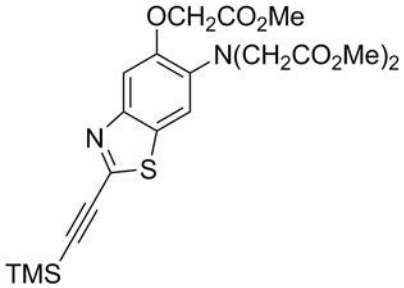

Synthesis of dimethyl 2,2'-((5-(2-methoxy-2-oxoethoxy)-2-((trimethylsilyl)ethynyl)benzo[d]thiazol-6-yl)azanediyl) diacetate (4)

To a solution of compound **3** (440 mg, 0.87 mmol) and triethylamine (1 mL) in dichloromethane (2 mL), was added ethynyltrimethylsilane (170 mg, 1.73 mmol), CuI (4 mg, 0.021 mmol), and $PdCl_2(PPh_3)_2$ (13 mg, 0.019 mmol) under inert atmosphere. The reaction mixture was refluxed for 1 h, then cooled to room temperature and filtered through a Celite pad. The filtrate was concentrated *in vacuo* and the residue was purified by column chromatography on silica gel (2:1 hexanes:EtOAc) to afford product **4** as a yellow solid (240 mg, 58%, R_f = 0.70 in 1:1 hexanes:EtOAc). M.p. 96-97 ºC. ^{1}H NMR (400 MHz, $CDCl_3$, δ): 0.29 (s, 9H), 3.75 (s, 6H), 3.79 (s, 3H), 4.27 (s, 4H), 4.72 (s, 2H), 7.28 (s, 1H), 7.37 (s, 1H). ^{13}C{^{1}H} NMR (100 MHz, $CDCl_3$, δ): -0.4, 52.1, 52.4, 53.9, 66.0, 77.4, 97.0, 107.1, 110.8, 129.5, 140.1, 147.0, 148.7, 150.5, 168.8, 171.6. ESI-MS (m/z): $[M+Na]^+$ calcd for $C_{21}H_{26}N_2O_7SSi$, 501.1; found 501.1.

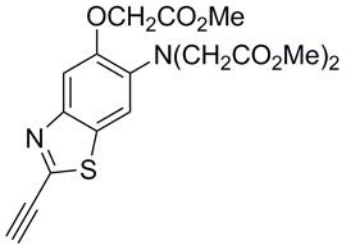

Synthesis of dimethyl 2,2'-((2-ethynyl-5-(2-methoxy-2-oxoethoxy)benzo[d]thiazol-6-yl)azanediyl)diacetate (5)

A mixture of compound **4** (230 mg, 0.48 mmol) and potassium fluoride (230 mg, 3.96 mmol) in methanol (4 mL) was stirred at room temperature for 1 h. The solvent was removed under vacuum and the residue was purified by column chromatography on silica gel (2:1 hexanes:EtOAc) to give product **5** as a white solid (150 mg, 77%, R_f = 0.52 in 1:1 hexanes:EtOAc). M.p. 111-113 °C. ^{1}H NMR (400 MHz, $CDCl_3$, δ): 3.55 (s, 1H), 3.74 (s, 6H), 3.79 (s, 3H), 4.28 (s, 4H), 4.72 (s, 2H), 7.29 (s, 1H), 7.39 (s, 1H). $^{13}C\{^1H\}$ NMR (100 MHz, $CDCl_3$, δ): 52.1, 52.4, 53.9, 66.0, 77.0, 83.6, 107.2, 110.7, 129.6, 140.3, 146.1, 148.4, 150.5, 168.7, 171.5. ESI-MS (m/z): $[M+Na]^+$ calcd for $C_{18}H_{18}N_2O_7S$, 429.1; found 429.1.

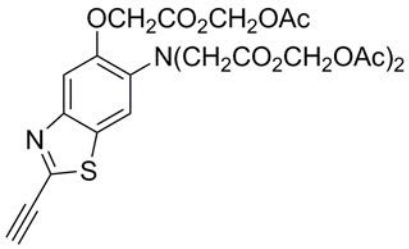

Synthesis of bis(acetoxymethyl) 2,2'-((5-(2-(acetoxymethoxy)-2-oxoethoxy)-2-ethynylbenzo[d] thiazol-6-yl)azanediyl)diacetate (5-AM)

A solution of ester **5** (120 mg, 0.30 mmol) in methanol (1.2 mL) was treated with aqueous potassium hydroxide (1.2 M, 1.2 mL, 1.44 mmol) and stirred at room temperature for 45 min. The solution was cooled in an ice bath and treated with cold, aqueous hydrochloric acid (2.0 M, 1.2 mL, 2.4 mmol). The resulting precipitate was collected by filtration, washed with cold 9:1 methanol:water (0.6 mL) followed by cold methanol (0.6 mL), and dried under vacuum. The product was suspended in 1:2 acetonitrile:chloroform (6 mL) and treated with diisopropyl ethylamine (478 μL, 355 mg, 2.74 mmol) followed by bromomethylacetate (488 μL, 762 mg, 4.98 mmol). The mixture was stirred at room temperature for 48 h protected from light and concentrated *in vacuo.* The residue was purified by column chromatography on silica gel (2:1 hexanes:EtOAc) to give compound **5-AM** as a white solid (60 mg, 35%, R_f = 0.48 in 1:1 hexanes:EtOAc). M.p. 46-47 °C. ^{1}H NMR (400 MHz, CD_2Cl_2, δ): 2.07 (s, 6H), 2.09 (s, 3H), 3.64 (s, 1H), 4.29 (s, 4H), 4.80 (s, 2H), 5.76 (s, 4H), 5.82 (s, 2H), 7.32 (s, 1H), 7.41 (s, 1H). $^{13}C\{^1H\}$ NMR (100 MHz, CD_2Cl_2, δ): 20.8, 20.9, 54.1, 65.9, 77.1, 79.68, 77.75, 83.8, 107.5, 111.4, 129.8, 139.9, 146.5, 148.9, 150.6, 167.6, 169.78, 169.84, 170.0. ESI-MS (m/z) $[M+Na]^+$ calcd for $C_{24}H_{24}N_2O_{13}S$, 603.1; found 603.1.

2.2. Syntheses of azides

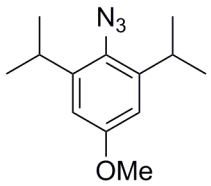

Synthesis of 2-azido-1,3-diisopropyl-5-methoxybenzene (8)

A solution of 2,6-diisopropyl-4-methoxyaniline (480 mg, 2.32 mmol) in acetonitrile (12 mL) was cooled to 0 °C, and treated with *tert*-butyl nitrite (1.10 mL, 955 mg, 9.26 mmol) followed by trimethylsilyl azide (922 μL, 800 mg, 6.95 mmol). The reaction mixture was stirred at room temperature for 1 h. The mixture was concentrated *in vacuo* and the residue was purified by column chromatography on silica gel (9:1 hexanes:EtOAc) to give azide **8** as a yellow liquid (473 mg, 86%, R_f = 0.85 in 9:1 hexanes:EtOAc).^{1}H NMR (400 MHz, $CDCl_3$, δ): 1.27 (d, *J* = 6.9 Hz, 12H), 3.35 (septet, *J* = 6.9 Hz, 2H), 3.81 (s, 3H), 6.67 (s, 2H). $^{13}C\{^1H\}$ NMR (100 MHz, $CDCl_3$, δ): 23.6, 29.2, 55.4, 109.4, 128.6, 144.7, 158.4. IR (neat): 2096, 2119 (N_3) cm^{-1}.

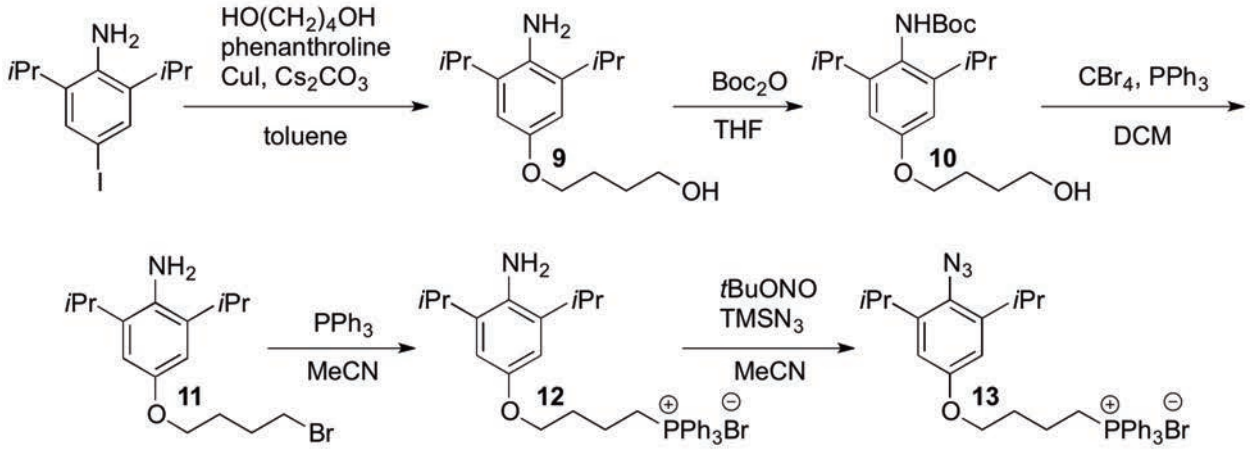

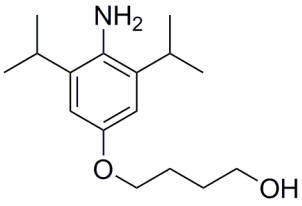

Synthesis of 4-(4-amino-3,5-diisopropylphenoxy)butan-1-ol (9)

A mixture of 4-iodo-2,6-diisopropylaniline (4.55 g, 15.0 mmol), CuI (571 mg, 3.0 mmol), 1,10-phenanthroline monohydrate (1.19 g, 6.0 mmol) and 1,4-butanediol (4.06 g, 45.0 mmol) in toluene (15 mL) was refluxed for 48 h under inert atmosphere. The resulting mixture was filtered through a short plug of silica gel, eluting with EtOAc. The filtrate was concentrated under vacuum, and the residue was purified by column chromatography on silica gel (3:1 hexanes:EtOAc) to give compound **9** as a white solid (2.38 g, 60%, R_f = 0.15 in 8:2 hexanes:EtOAc). M.p. 54-55 °C. ^{1}H NMR (400 MHz, CD_3OD, δ): 1.23 (d, *J* = 6.8 Hz, 12H), 1.66-1.74 (m, 2H), 1.75-1.84 (m, 2H), 3.04 (septet, *J* = 6.8 Hz, 2H), 3.62 (t, *J* = 6.4 Hz, 2H), 3.92 (t, *J* = 6.3 Hz, 2H), 6.59 (s, 2H). ^{13}C{^{1}H} NMR (100 MHz, CD_3OD, δ): 23.2, 27.2, 28.9, 30.3, 62.8, 69.4, 110.6, 134.8, 136.3, 154.0. ESI-MS (m/z): $[M+H]^+$ calcd for $C_{16}H_{27}NO_2$, 266.2; found, 266.1.

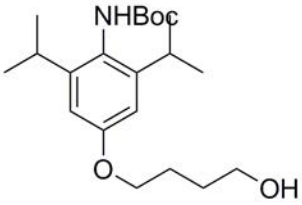

Synthesis of *tert*-butyl (4-(4-hydroxybutoxy)-2,6-diisopropyl phenyl)carbamate (10)

A solution of compound **9** (1.06 g, 4.0 mmol) in THF (4 mL) was cooled to 0 °C, treated with di-*tert*-butyl dicarbonate (960 mg, 4.4 mmol) and then stirred at room temperature overnight. The solvent was removed under vacuum to yield an oil, which was triturated in ethyl acetate:hexane (15:85) to give the compound **10** as a colorless crystals (1.36 g, 93%, R_f = 0.17 in 8:2 hexanes:EtOAc). M.p. 136-137 °C. ^{1}H NMR (400 MHz, DMSO-d_6, δ) two conformers were observed in a ~8:2 ratio. Major conformer: 1.11 (d, *J* = 6.8 Hz, 12H), 1.43 (s, 9H), 1.53-1.60 (m, 2H), 1.70-1.77 (m, 2H), 3.03-3.10 (m, 2H), 3.46 (td, *J* = 6.3 Hz, *J* = 5.2 Hz, 2H), 3.96 (t, *J* = 6.4 Hz, 2H), 4.43 (t, *J* = 5.2 Hz, 1H), 6.61 (s, 1H), 8.11 (s, 1H,). Minor conformer: 1.11 (d, *J* = 6.8 Hz, 12H), 1.27 (s, 9H), 1.53-1.60 (m, 2H), 1.70-1.77 (m, 2H), 3.03-3.10 (m, 2H), 3.46 (td, *J* = 6.3 Hz, *J* = 5.2 Hz, 2H), 3.96 (t, *J* = 6.4 Hz, 2H), 4.43 (t, *J* = 5.2 Hz, 1H), 6.61 (s, 1H), 7.81 (s, 1H). ^{13}C{^{1}H} NMR (100 MHz, DMSO-d_6, δ) for major conformer: 23.1. 23.4, 25.5, 28.1, 28.2, 29.0, 60.4, 67.2, 77.8, 108.6, 125.3, 147.9, 155.1, 157.7. ESI-MS (m/z): $[M+Na]^+$ calcd for $C_{21}H_{35}NO_4$, 388.2; found 388.2.

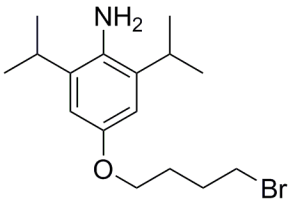

Synthesis of 4-(4-bromobutoxy)-2,6-diisopropylaniline (11)

A solution of compound **10** (731 mg, 2.0 mmol) in dichloromethane (10 mL) was treated with acetone (0.1 mL), CBr_4 (1.33 g, 4.0 mmol), and then triphenylphosphine (1.05 g, 4.0 mmol) was added in portions. The reaction solution was stirred at room temperature for 1 h and concentrated under vacuum. The residue was purified by column chromatography on silica gel (8:2 hexanes:EtOAc) to give compound **11** as a colorless oil (360 mg, 55%, R_f = 0.59 in 8:2 hexanes:EtOAc). ^{1}H NMR (400 MHz, CD_3OD, δ): 1.23 (d, *J* = 6.8 Hz, 12H), 1.83-1.93 (m, 2H), 1.98-2.06 (m, 2H), 3.03 (septet, *J* = 6.8 Hz, 2H), 3.50 (t, *J* = 6.6 Hz, 2H), 3.93 (t, *J* = 6.2 Hz, 2H), 6.59 (s, 2H). ^{13}C{^{1}H} NMR (100 MHz, CD_3OD, δ): 23.2, 28.9, 29.3, 30.8, 34.2, 68.6, 110.6, 134.6, 136.4, 153.9. ESI-MS (m/z): $[M+H]^+$ calcd for $C_{16}H_{26}BrNO$, 328.1; found, 328.1.

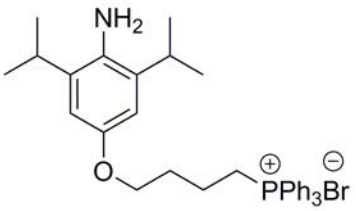

Synthesis of (4-(4-amino-3,5-diisopropylphenoxy)butyl) triphenylphosphonium bromide (12)

A mixture of compound **11** (400 mg, 1.22 mmol) and PPh_3 (956 mg, 3.66 mmol) in acetonitrile (2.5 mL) was heated to 80 °C overnight in a sealed vial. After allowing to cool to room temperature, the reaction mixture was added to Et_2O (25 mL) to yield a white precipitate. The solid was collected and purified by chromatography on neutral alumina (9:1 EtOAc:MeOH) to afford product **12** as a white solid (480 mg, 67%, R_f = 0.35 in 8:2 EtOAc:MeOH). M.p. 95 °C (dec). ^{1}H NMR (400 MHz, CD_3OD, δ): 1.20 (d, *J* = 6.8 Hz, 12H), 1.80-1.94 (m, 2H), 1.94-2.03 (m, 2H), 3.04 (septet, *J* = 6.8 Hz, 2H), 3.46-3.53 (m, 2H), 3.93-4.05 (m, 2H), 6.54 (s, 2H), 7.70-7.82 (m, 12H), 7.85-7.90 (m, 3H). ^{13}C{^{1}H} NMR (100 MHz, CD_3OD, δ): 20.6 (d, *J* = 4.0 Hz), 22.3 (d, *J* = 51.5 Hz), 23.2, 28.9, 30.9 (d, *J* = 16.2 Hz), 67.7, 110.4, 119.9 (d. *J* = 85.9 Hz), 131.5 (d, *J* = 12.5 Hz), 134.8 (d, *J* = 9.9 Hz), 135.0, 136.3 (d, *J* = 3.0 Hz), 136.4, 153.5. ^{31}P NMR (162 MHz, CD_3OD, δ): 25.61. ESI-MS (m/z): $[M]^+$ calcd for $C_{34}H_{41}NOP$, 510.3; found 510.2.

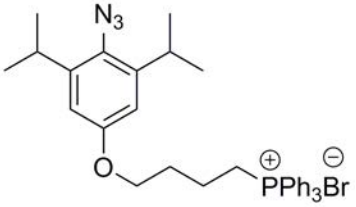

Synthesis of (4-(4-azido-3,5-diisopropylphenoxy)butyl) triphenylphosphonium bromide (13)

A solution of compound **12** (480 mg, 0.81 mmol) in acetonitrile was cooled to 0 °C and treated with *tert*-butylnitrite (386 μL, 335 mg, 3.25 mmol) followed by trimethylsilylazide (324 μL, 281 mg, 2.44 mmol). The reaction mixture was stirred at room temperature for 2 h. The solvent was removed *in vacuo* and the residue was purified by column chromatography on neutral alumina (9:1 EtOAc:MeOH) to yield compound **13** as a white solid (430 mg, 86%, R_f = 0.39 in 8:2 EtOAc:MeOH). M.p. 101 °C (dec). ^{1}H NMR (400 MHz, CD_3OD, δ) 1.23 (d, *J* = 6.9 Hz, 12H), 1.84-1.94 (m, 2H), 1.99-2.05 (m, 2H), 3.31 (m overlapping solvent, 2H), 3.47-3.55 (m, 2H), 4.05 (t, *J* = 5.8 Hz, 2H), 6.64 (s, 2H), 7.71-7.83 (m, 12H), 7.87-7.91 (m, 3H). ^{13}C{^{1}H} NMR (100 MHz, CD_3OD, δ): 20.4 (d, *J* = 4.1 Hz), 22.3 (d, *J* = 51.1 Hz), 23.8, 30.3, 30.9 (d, *J* = 16.2 Hz), 67.5, 111.1, 119.9 (d. *J* = 85.8 Hz), 129.8, 131.5 (d, *J* = 12.5 Hz), 134.8 (d, *J* = 9.9 Hz), 136.3 (d, *J* = 3.0 Hz), 145.8, 159.0. ^{31}P NMR (162 MHz, CD_3OD, δ): 27.16. ESI-MS (m/z): $[M]^+$ calcd for $C_{34}H_{39}N_3OP$, 536.3; found 536.2. IR (neat): 2096, 2119 (N_3) cm^{-1}.

2.3. Assembly of triazole-containing sensors

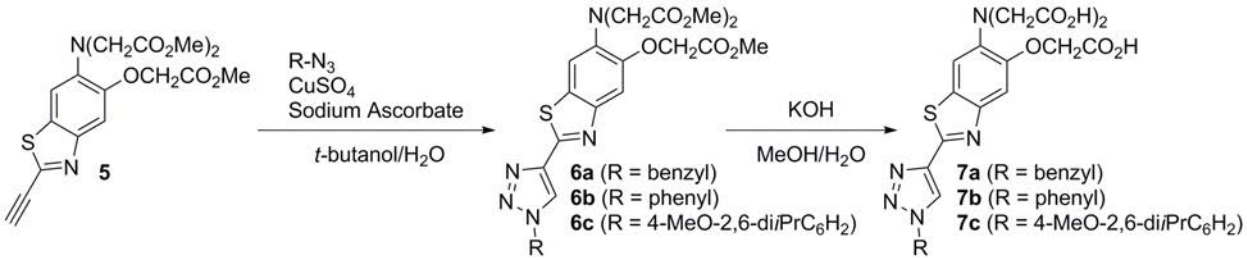

General procedure for the synthesis of methyl esters 6a-c
A suspension of alkyne **5** (50 mg/mL) and azide (1.2 equiv) in a 1:1 mixture of water and *tert*-butanol was treated with sodium ascorbate (0.2 equiv), followed by $CuSO_4 \cdot 5H_2O$ (0.1 equiv). The suspension was stirred vigorously overnight. The reaction mixture was diluted with water and then extracted with EtOAc. The combined organics were washed with dilute NH_4OH followed by water, then dried over Na_2SO_4, and concentrated *in vacuo*. The residue was purified by column chromatography on silica gel (1:1 hexanes:EtOAc).

Compound 6a White solid (48% yield from 150 mg of alkyne. R_f = 0.18 in 1:1 hexanes:EtOAc). M.p. 187-188 °C. ^{1}H NMR (400 MHz, $CDCl_3$, δ): 3.75 (s, 6H), 3.78 (s, 3H), 4.28 (s, 4H), 4.72 (s, 2H), 5.60 (s, 2H), 7.33-7.41 (m, 7H), 8.07 (s, 1H). ^{13}C{^{1}H} NMR (100 MHz, $CDCl_3$, δ): 52.1, 52.4, 54.0, 54.8, 66.1, 107.0, 111.8, 121.6, 128.6, 128.8, 129.3, 129.5, 133.9, 139.1, 143.8, 149.3, 150.3, 158.4, 168.9, 171.6. HR-TOF-MS (m/z): $[M+H]^+$ calcd for $C_{25}H_{25}N_5O_7S$, 540.15474; found 540.15468. Anal. calcd for $C_{25}H_{25}N_5O_7S$: C, 55.65; H, 4.67; N, 12.98. Found: C, 55.41; H, 4.74; N, 12.79.

Compound 6b White solid (86% yield from 100 mg of alkyne. R_f = 0.23 in 1:1 hexanes:EtOAc). M.p. 171-172 °C. ^{1}H NMR (400 MHz, $CDCl_3$, δ): 3.76 (s, 6H), 3.81 (s, 3H), 4.30 (s, 4H), 4.76 (s, 2H), 7.42 (s, 1H), 7.44 (s, 1H), 7.49 (m, 1H), 7.58 (m, 2H), 7.81 (m, 2H), 8.61 (s, 1H). ^{13}C{^{1}H} NMR (100 MHz, $CDCl_3$, δ): 52.1, 52.4, 54.0, 66.2, 107.1, 111.8, 119.6, 120.8, 129.0, 129.5, 130.1, 136.8, 139.3, 144.1, 150.4, 158.0, 169.0, 171.6. HR-TOF-MS (m/z): $[M+H]^+$ calcd for $C_{24}H_{23}N_5O_7S$, 526.13909; found 526.13906. Anal. calcd for $C_{24}H_{23}N_5O_7S$: C, 54.85; H, 4.41; N, 13.33. Found: C, 55.00; H, 4.29; N, 13.20.

Compound 6c White solid (85% yield from 36 mg of alkyne. R_f = 0.48 in 1:1 hexanes:EtOAc). M.p. 174-175 °C. ^{1}H NMR (400 MHz, CD_2Cl_2, δ): 1.14 (d, *J* = 6.8 Hz, 6H), 1.15 (d, *J* = 6.8 Hz, 6H), 2.29 (septet, *J* = 6.8 Hz, 2H), 3.73 (s, 6H), 3.79 (s, 3H), 3.89 (s, 3H), 4.27 (s, 4H), 4.76 (s, 2H), 6.83 (s, 2H), 7.40 (s, 1H), 7.45 (s, 1H), 8.27 (s, 1H). ^{13}C{^{1}H} NMR (100 MHz, CD_2Cl_2, δ): 24.0, 24.3, 29.1, 52.1, 52.5, 54.1, 55.9, 66.3, 107.2, 109.6, 112.0, 125.4, 126.2, 128.9, 139.4, 143.5, 148.1, 149.6, 150.5, 158.6, 161.9, 169.2, 171.7. HR-TOF-MS (m/z): $[M+H]^+$ calcd for $C_{31}H_{37}N_5O_8S$, 640.24356; found 640.24344. Anal. calcd for $C_{31}H_{37}N_5O_8S$: C, 58.20; H, 5.83; N, 10.95. Found: C, 57.98; H, 5.81; N, 10.80.

General procedure for the quantitative hydrolysis of esters 6a-c: preparation of 7a-c
A quantitative sample of ester **6a-c** (0.0100 mmol) in methanol (100 µL) was treated with aqueous potassium hydroxide (100 µL, 1.2 M, 0.12 mmol) and stirred at room temperature for 24 h. The solution was transferred quantitatively to a volumetric flask and diluted with buffer at pH 7.0 (50 mM PIPES, 100 mM KCl) to a final concentration of 2.00 mM. The stock solution was divided into small aliquots, flash frozen in liquid nitrogen, and stored below -20 °C.

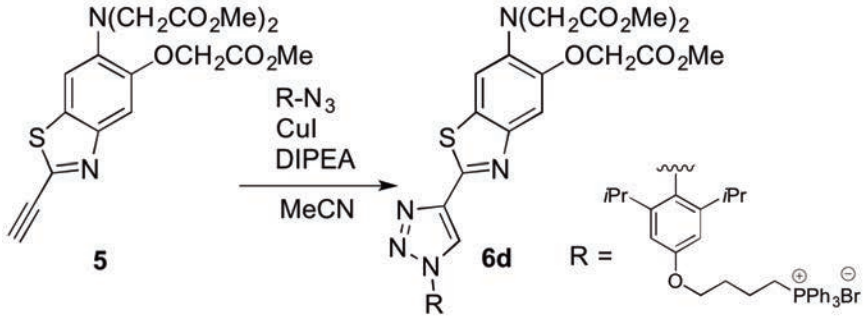

Synthesis of methyl ester 6d

A solution of alkyne **5** (20 mg, 0.049 mmol), azide **13** (36 mg, 0.059 mmol), CuI (0.5 mg, 0.0026 mmol), and diisopropylethyamine (26 uL, 0.15 mmol) in CH_3CN (3.0 mL) was stirred under nitrogen at room temperature for 4 h. The solvent was removed *in vacuo* and the residue was purified by column chromatography on neutral alumina (50:1 DCM:MeOH) to give compound **6d** as a white solid (15 mg, 32%, R_f = 0.27 in 50:1 DCM:MeOH). M.p. 210 °C (dec). ^{1}H NMR (400 MHz, CD_3CN, δ): 1.10 (d, *J* = 6.8 Hz, 6H), 1.13 (d, *J* = 6.8 Hz, 6H), 1.80-1.91 (m, 2H), 1.96-2.04 (m, 2H), 2.19-2.29 (m, 2H), 3.30-3.38 (m, 2H), 3.69 (s, 6H), 3.75 (s, 3H), 4.13 (t, *J* = 6.0 Hz, 2H), 4.25 (s, 4H), 4.81 (s, 2H), 6.83 (s, 2H), 7.43 (s, 1H), 7.51 (s, 1H), 7.68-7.77 (m, 12H), 7.85-7.90 (m, 3H), 8.51 (s, 1H). ^{13}C{^{1}H} NMR (100 MHz, CD_3CN, δ): 19.9 (d, *J* = 3.7 Hz), 22.3 (d, *J* = 51.9 Hz), 23.9, 24.2, 29.6, 30.3 (d, *J* = 16.7 Hz), 52.3, 52.8, 54.4, 66.6, 67.6, 107.7, 110.7, 112.2, 119.3 (d, *J* = 86.4 Hz), 126.5, 126.8, 129.0, 131.3 (d, *J* = 12.6 Hz), 134.7 (d, *J* = 10.0 Hz), 136.2 (d, *J* = 3.0 Hz), 139.9, 144.1, 148.8, 150.0, 150.9, 158.7, 161.7, 170.1, 172.2. ^{31}P NMR (162 MHz, CD_3CN, δ): 27.05. HR-TOF-MS (m/z): $[M]^+$ calcd for $C_{52}H_{57}N_5O_8PS$, 942.36600; found 942.36535.

Preparation of stock solution of Mag-*mito* free acid for spectroscopic characterization

The general procedure described for the quantitative hydrolysis of esters **6a-c** was employed here for the quantitative hydrolysis of **Mag-*mito*** methyl ester, compound **6d**.

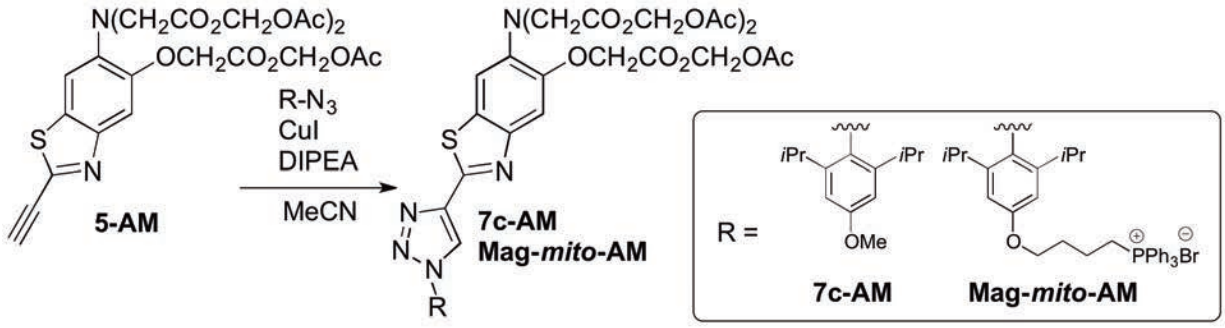

General procedure for the synthesis of acetoxymethyl esters 7c-AM and Mag-*mito*-AM

A solution of alkyne **5-AM** (20 mM), azide (1.5 equiv), CuI (0.2 equiv), and diisopropylethyamine (2.0 equiv) in CH_3CN was stirred under nitrogen at room temperature for 6 h. The solvent was removed *in vacuo*, and the residue was purified by chromatography.

Compound 7c-AM Purified by column chromatography on silica gel (1:1 hexanes:EtOAc) to yield a white solid (86% starting from 20 mg alkyne. R_f = 0.63 in 1:1 hexanes:EtOAc). M.p. 136-

137 °C. ^{1}H NMR (400 MHz, CD_2Cl_2, δ): 1.14 (d, *J* = 6.8 Hz, 6H), 1.15 (d, *J* = 6.8 Hz, 6H), 2.09 (s, 9H), 2.29 (septet, *J* = 6.8 Hz, 2H), 3.89 (s, 3H), 4.31 (s, 4H), 4.82 (s, 2H), 5.78 (s, 4H), 5.82 (s, 2H), 6.83 (s, 2H), 7.42 (s, 1H), 7.46 (s, 1H), 8.27 (s, 1H). ^{13}C{^{1}H} NMR (100 MHz, CD_2Cl_2, δ): 20.8, 20.9, 24.0, 24.3, 29.1, 30.1, 55.9, 66.1, 79.7, 79.8, 107.4, 109.7, 112.5, 125.5512, 125.5516, 126.1, 129.1, 138.9, 148.1, 150.5, 159.1, 162.0, 167.8, 169.8, 169.9, 170.1. HR-TOF-MS (m/z): $[M+H]^+$ calcd for $C_{37}H_{43}N_5O_{14}S$, 814.26000; found 814.26002.

Compound Mag-*mito*-AM Purified by C18 reversed-phase preparative TLC, eluting three times (8:2 acetonitrile:water) to yield a pale yellow solid (28% starting from 40 mg of alkyne. R_f = 0.06 in 8:2 acetonitrile:water). ^{1}H NMR (400 MHz, CD_3OD, δ): 1.14 (d, *J* = 6.8 Hz, 6H), 1.16 (d, *J* = 6.8 Hz, 6H), 1.88-1.99 (m, 2H), 2.05 (s, 3H), 2.06 (s, 6H), 2.00-2.14 (m, 2H), 2.18-2.31 (m, 2H), 3.51-3.58 (m, 2H), 4.17 (t, *J* = 5.7 Hz, 2H), 4.33 (s, 4H), 4.91 (s, 2H), 5.80 (s, 4H), 5.83 (s, 2H), 6.85 (s, 2H), 7.50 (s, 1H), 7.59 (s, 1H), 7.73-7.92 (m, 15H), 8.74 (s, 1H). ^{31}P NMR (162 MHz, CD_3OD, δ): 27.19. HR-TOF-MS (m/z): $[M]^+$ calcd for $C_{58}H_{63}N_5O_{14}PS$, 1116.38244; found 1116.38198.

3. Spectroscopic Methods

All aqueous solutions were prepared using de-ionized water having a resistivity of ≥18 MΩ cm. Other solvents were supplied by commercial vendors and used as received. Piperazine-N,N-bis(2-ethanesulfonic acid) (PIPES), 99.999% KCl, 99.999% $MgCl_2$, 99.99% $CaCl_2$, and high-purity 25% HCl, 45% KOH, 50% NaOH, and other metal salts were purchased from Sigma Aldrich. Other reagents were acquired from various vendors and used as received. Stock solutions of the sensors in their acid form were stored at -20 °C and thawed immediately before each experiment. Measurements at pH 7.0 were conducted in aqueous buffer containing 50 mM PIPES and 100 mM KCl. Buffers were treated with Chelex resin (Bio-Rad) according to the manufacturer's protocol, to remove adventitious metal ions unless otherwise noted. Measurements of pH were conducted using a Mettler Toledo FE20 with glass electrode. UV-visible spectra were acquired on a Cary 100 spectrophotometer using quartz cuvettes from Starna (1 cm path length). Fluorescence spectra were acquired on a QuantaMaster 40 Photon Technology International spectrofluorometer equipped with xenon lamp source, emission and excitation monochromators, excitation correction unit, and PMT detector. Emission spectra were corrected for the detector wavelength-dependent response. The excitation spectra were corrected for the wavelength-dependent lamp intensity. All measurements were conducted at 25.0 ± 0.2 °C. Extinction coefficients were determined using sensor solutions in the 0-11 μM range in aqueous buffer at pH 7.0, in the absence or presence of 200 mM Mg^{2+} for the metal-free and -bound forms, respectively. Fluorescence quantum yields were determined using 0.5-3.0 μM solutions of the sensor in aqueous buffer at pH 7.0, exciting at the reported excitation maxima for each compound. Solutions of quinine in 0.5 M aqueous sulfuric acid, with a reported quantum yield of 0.546 upon excitation at 347 nm, were used as standards.[5] Fluorescence emission spectra were integrated from 360 to 680 nm.

Metal selectivity study

Metal selectivity measurements were conducted using solutions of the sensors in aqueous buffer at pH 7.0 (10 μM for **7b**, 2 μM for **7a** and **7c**) treated with either $CaCl_2$, $MnCl_2$, $(NH_4)_2Fe(SO_4)_2$, $CoCl_2$, $NiCl_2$, $CuCl_2$, or $ZnCl_2$ in aqueous buffer for a final concentration of 5 μM M^{n+}, and then 50 μM M^{n+}, or 50 μM M^{n+} with 200 mM $MgCl_2$.

Study of pH-dependent response

The pH response study was conducted using 1 μM solution of compound **7c** in aqueous buffer at pH ranging from 5.5 to 8.0. Aqueous MES buffers (100 mM KCl, 50 mM MES) were used in the pH range from 5.5 to 6.5. Aqueous HEPES buffers (100 mM KCl, 50 mM HEPES) were used in the pH range from 7.0 to 8.0. For measurements of the ratio in the metal-free form, 5 μM of EDTA was applied to chelate residual metals. For the metal-saturated experiment, measurements were conducted in the presence of 200 μM $MgCl_2$.

Determination of metal dissociation constants

Fluorescence titrations were conducted using 5 μM of compound **7b**, and 2 μM solutions of compounds **7a**, **7c** and **Mag-*mito*** in aqueous buffer at pH 7.0, with increasing concentrations of Mg^{2+} or Ca^{2+} spanning the range 0-500 mM for $[Mg^{2+}]_t$ and 0-2 mM for $[Ca^{2+}]_t$. Excess metal was employed to confirm the saturation value. Magnesium was added from a 1000 mM $MgCl_2$ stock solution. Calcium was added from 10 or 1000 mM $CaCl_2$ stock solutions. For each titration, the metal solution was treated with an appropriate amount of the sensor to match the concentration in the cuvette and prevent sensor dilution throughout the experiment.

For compound **7b**, the apparent K_d value for magnesium dissociation was determined using equation S1, where F is the fluorescence intensity at any point, F_{min} is the fluorescence intensity before addition of metal, and F_{max} is the fluorescence intensity at saturation.

$$[Mg^{2+}] = K_d \frac{F - F_{min}}{F_{max} - F} \qquad \text{(S1)}$$

For compounds **7a**, **7c** and **Mag-*mito***, apparent K_d values for magnesium dissociation were obtained using equation S2,[6] where R is the ratio of fluorescence intensity upon excitation at two wavelengths ($R=I_{\lambda 1}/I_{\lambda 2}$), R_{min} is the fluorescence ratio for the metal-free sensor, R_{max} is the fluorescence ratio of the metal-saturated sensor, and S_{f2} and S_{b2} are proportionality coefficients for the fluorescence of the metal-free and -bound forms of the sensor, respectively, upon excitation at λ_2.

$$[Mg^{2+}] = K_d \frac{R - R_{min}}{R_{max} - R} \frac{S_{f2}}{S_{b2}} \qquad \text{(S2)}$$

Linear fits of plots of $(F_{max}-F)/(F-F_{min})$ or $(R_{max}-R)/(R-R_{min})$ vs. $1/[Mg^{2+}]$ were employed, using the approximation $[Mg^{2+}] \approx [Mg^{2+}]_t$. Reported K_d values correspond to averages of three independent titrations.

Apparent K_d values for calcium dissociation were obtained from non-linear fit of the fluorescence ratio R versus total calcium concentration according to equation S3, with values of $[Ca^{2+}]$ obtained by solving simultaneously equation S4.[7] Reported K_d values correspond to averages of three independent titrations.

$$R = \frac{R_{max}[Ca^{2+}] + R_{min}(K_d S_{f2} / S_{b2})}{[Ca^{2+}] + (K_d S_{f2} / S_{b2})} \qquad \text{(S3)}$$

$$[Ca^{2+}] + \left([Sensor]_t - [Ca^{2+}]_t + K_d\right)[Ca^{2+}] - K_d[Ca^{2+}]_t = 0 \qquad \text{(S4)}$$

Study of Mg^{2+} sensing behavior in the presence of adenosine triphosphate (ATP)

Fluorescence titration was conducted using solution of compound **7c** (2 μM) and ATP (18.4 mM) in aqueous buffer at pH 7.0, with increasing concentrations of Mg^{2+} spanning the range 0-120 mM for $[Mg^{2+}]_t$. Magnesium was added from a 1000 mM $MgCl_2$ stock solution. The magnesium solution was treated with an appropriate amount of sensor **7c** and ATP to match the concentrations in the cuvette and prevent dilution throughout the experiment.

4. Cell culture and imaging protocols

HeLa cells were incubated in Dulbecco's Modified Eagle Medium (DMEM) supplemented with 10% fetal bovine serum (FBS) at 37 °C in 5% CO2 humidified atmosphere. Cells were seeded in 35 mm glass bottom cell culture dishes and allowed to grow to 40-60% confluence prior to imaging. Plasmid for genetically encoded calcium indicator (pcDNA-4mtD3cpv,[8] Addgene plasmid # 36324) was purified using an Endo-Free Plasmid Maxi Kit (Qiagen) prior to transfection. Fluorescence spectra of sensor-loaded cells were acquired on 96-well half-area plates (Costar) using a Molecular Devices FlexStation 3 Multi-Mode Microplate Reader. Fluorescence imaging experiments were performed on a Leica DMI6000B inverted fluorescence microscope equipped with a Hamamatsu ORCA-Flash 4.0 CCD camera, Tokai Hit stage-top incubator, scanning stage, high-speed filter wheel for excitation filters and a mercury metal halide external light source. A Fura-2 filter set from Leica was employed for ratiometric imaging of the magnesium sensor. A CFP-YFP FRET filter set was employed for imaging the genetically encoded calcium indicator. A Leica GFP filter cube was employed for the imaging of Mitotracker Green and a TX Red cube was employed for imaging of ethidium homodimer-1. Crosstalk experiments were conducted with the various filter/dye combinations, ruling out bleed-through of the Mitotracker Green signal into the magnesium indicator channels and viceversa. The microscope was operated with Leica LAS AF software version 3.2.0.9652. Image processing for ratio determination was performed with Metamorph 7.7.0.0 software. Deconvolution of z-stacked images was performed with Autoquant X3.0.2 using iterative restoration algorithms; co-localization analysis was performed over the reconstructed cell volumes. Concentrations of free Mg^{2+} were calculated from fluorescence ratio values following equation S2. Values of R_{max} and R_{min} were obtained through a procedure adapted from Trapani *et al*.[9] Briefly, HeLa cells were lysed with 40 μM digitonin and 1% (w/v) SDS, and the lysate was treated with 1 μM Mag-*mito* or non-targeted 7c and either 200 mM $MgCl_2$ (R_{max}) or 50 mM EDTA (R_{min}). Each lysate (5 μL) was placed on a coverslip and mounted on a microscope slide. Images were collected using the same exposure times as the corresponding experiments to be calibrated. Images from a sample of lysate without sensor were employed for background subtraction. The K_d at 37 °C was re-determined on the microscope by conducting magnesium titrations of 1 μM sensor in buffer, treated in a 35 mm glass-bottom dish with increasing concentrations of Mg^{2+} ranging from 0 to 200 mM.

Imaging of magnesium in HeLa cells

For loading the magnesium sensors, cells were washed with FBS-free DMEM (2 mL) and then incubated at room temperature for 30 min in FBS-free DMEM (2 mL) containing 1 μM **Mag-*mito*-AM** suspended with Pluronic F-127 according to manufacturers protocol or 1 μM **7c-AM**. After loading, the medium was replaced with fresh FBS-free DMEM (2 mL) and cells were allowed to stand for an additional 30 min at room temperature to complete de-esterification of the sensor. Prior to imaging, the cells were washed with Hank's balanced salt solution (HBSS)

or FluoroBrite DMEM (Life Technologies) (2 mL) and bathed in HBSS or FluoroBrite (1 mL) for image acquisition. To confirm the sensor's response to Mg^{2+}, cells were treated on the microscope stage with medium supplemented with additional $MgCl_2$ and non-fluorescent ionophore 4-bromo A-23187 (Molecular Probes) for a total concentration of 20 mM and 2.5 μM, respectively. For comparison, images before and after treatment with excess magnesium and ionophore were acquired and processed under identical conditions, and are shown on the same ratio scale. Background subtraction and threshold was applied on individual channel images prior to ratio calculation. For co-localization analysis, cells were incubated in FBS-free DMEM (2 mL) containing MitoTracker Green FM (50 nM, Molecular Probes) for 15 minutes at 37 °C and washed prior to loading the magnesium indicator. Z-sectioned images at 0.2 μm intervals were employed to discern possible effects of organelle overlap along the z-axis.

Sensing of Mg^{2+} in HeLa cells

HeLa cells were grown on a 100 mm dish and loaded with 6 μM **7c-AM** as described above. Following loading and de-esterification steps, cells were washed with PBS, detached by scraping, and pelleted at 850 x g for 3 minutes. The pellet was resuspended in HBSS and aliquoted into micro wells of a 96-well black half-area plate. The excitation spectrum was collected on a plate reader. A sample incubated for 30 min with 2.5 μM 4-Bromo A-23187 and 50 mM EDTA was employed to verify the response of the sensor to decreasing concentrations of intracellular Mg^{2+}.

Imaging of mitochondrial magnesium in apoptotic HeLa cells

Cells were treated with **Mag-*mito*-AM** (1 μM) and Mitotracker Green (50 nM) as described in the general imaging protocol. During the de-esterification period, cells were allowed to stand at 25 °C for 30 minutes in FBS-free FluoroBrite DMEM (1 mL) that contained the caspase indicator CellEvent Caspase 3/7 (Life Technologies) per manufacturers protocol, and ethidium homodimer-1 (Ethd-1, 1 μM) necrosis stain. Cells were maintained at 37 °C and under 5% CO_2 humidified atmosphere on the microscope stage for the duration of the imaging experiment. Staurosporine (4 mM in DMSO stock, Life Technologies) was diluted to a final concentration of 2 μM in FBS-free FluoroBrite DMEM (1 mL) containing CellEvent Caspase 3/7 and Ethd-1. The warm solution was applied to the imaging dish on the microscope stage to induce apoptosis. Images were collected every 5 minutes for the first 30 minutes followed by every 10 minutes for a total of 2 hours. Background subtraction and threshold was applied on individual channel images prior to ratio calculation.

To rule out potential interference from Zn^{2+} in the detection of Mg^{2+}, a control experiment was conducted in which 10 μM of zinc chelator tris-(2-pyridylmethyl)amine (TPA, K_d = 10 pM) was added to the culture dish 15 minutes after induction of apoptosis in cells treated with **Mag-*mito*-AM** as described above. Image acquisition and processing was conducted in a similar fashion.

Imaging of mitochondrial calcium in apoptotic HeLa cells

Cells were transfected using Lipofectamine 3000 (Life Technologies) per manufacturers protocol and imaged 2 days after transfection. Right before imaging, cells were washed (1×2 mL) and then bathed (1 mL) with FBS-free FluoroBrite DMEM. To induce apoptosis, staurosporine (4 mM in DMSO stock) was diluted to a final concentration of 2 μM in FBS-free FluoroBrite DMEM (1 mL) and applied to the cell dish on the microscope stage. Images were collected every 2 minutes for the first 20 minutes followed by every 5 minutes for a total of 2 hours. Image processing was conducted following protocols described by Palmer and Tsien. [10]

5. NMR spectroscopic data for new sensors

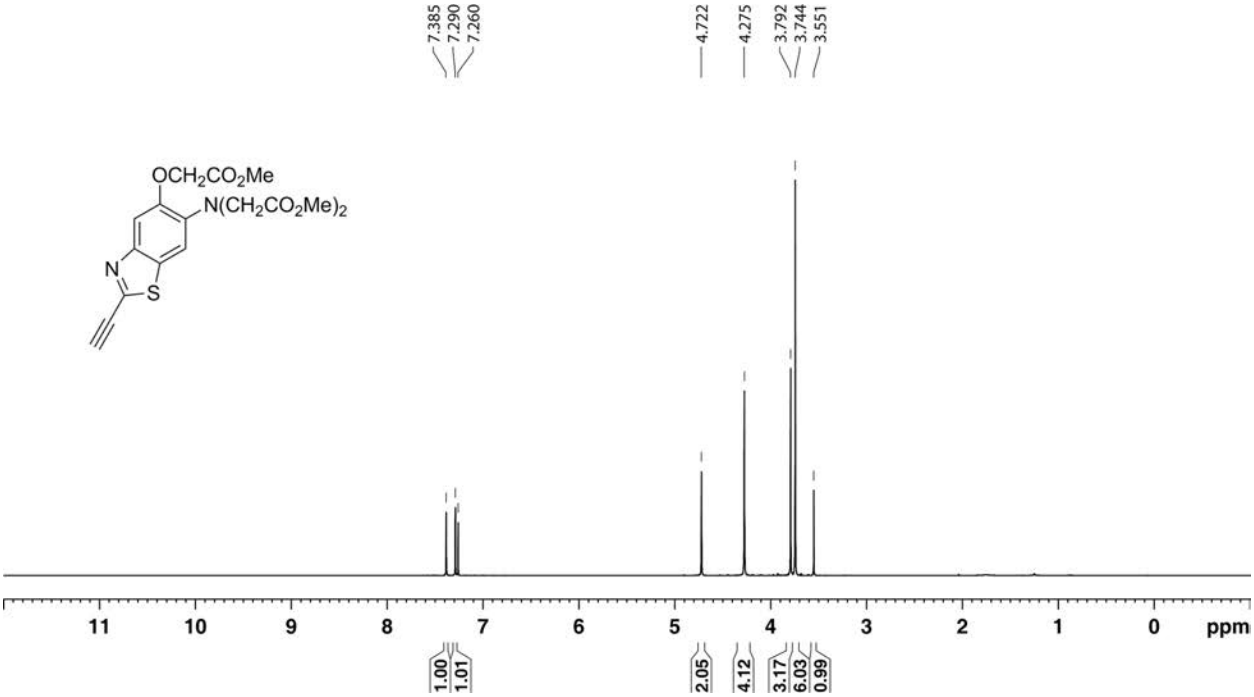

Figure S19. ^{1}H NMR spectrum of compound **5**, in $CDCl_3$.

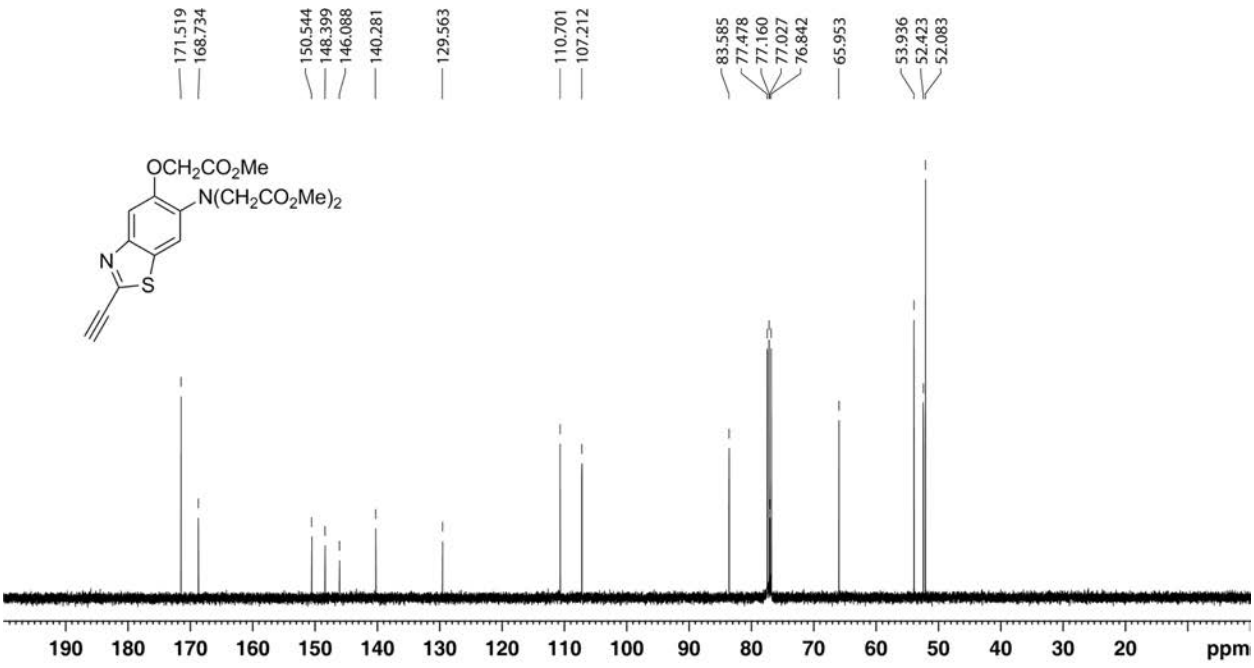

Figure S20. $^{13}C\{^{1}H\}$ NMR spectrum of compound **5**, in $CDCl_3$.

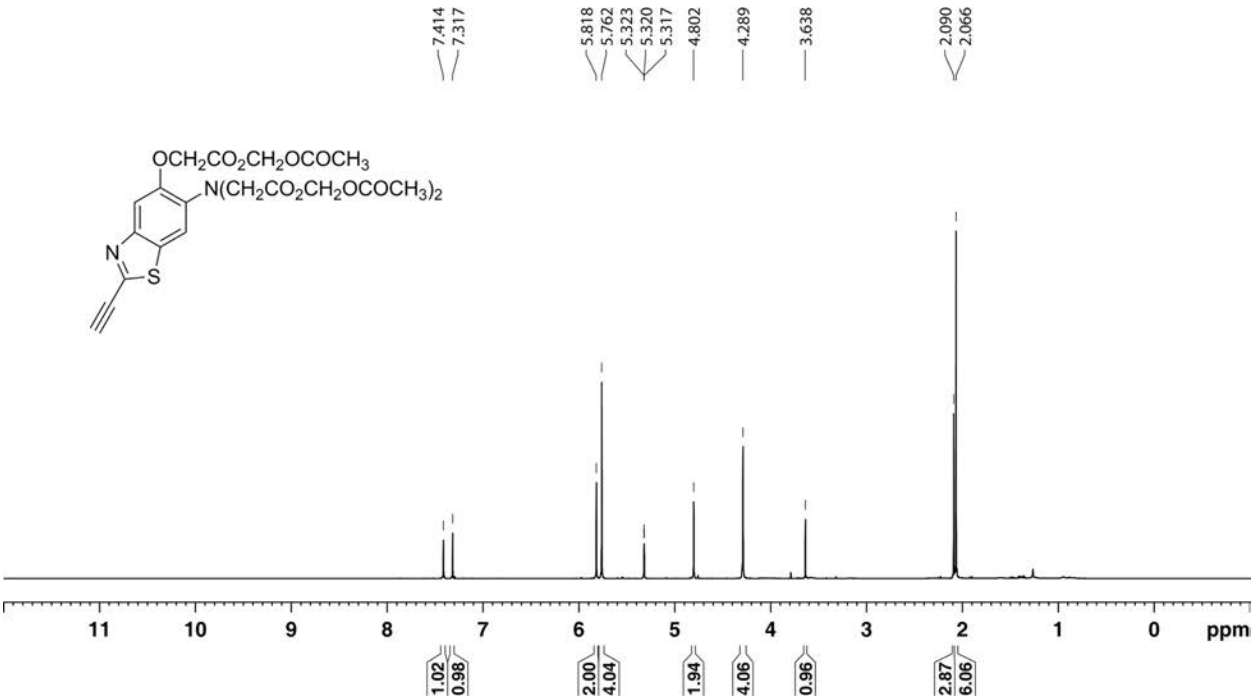

Figure S21. ^{1}H NMR spectrum of compound **5-AM**, in CD_2Cl_2.

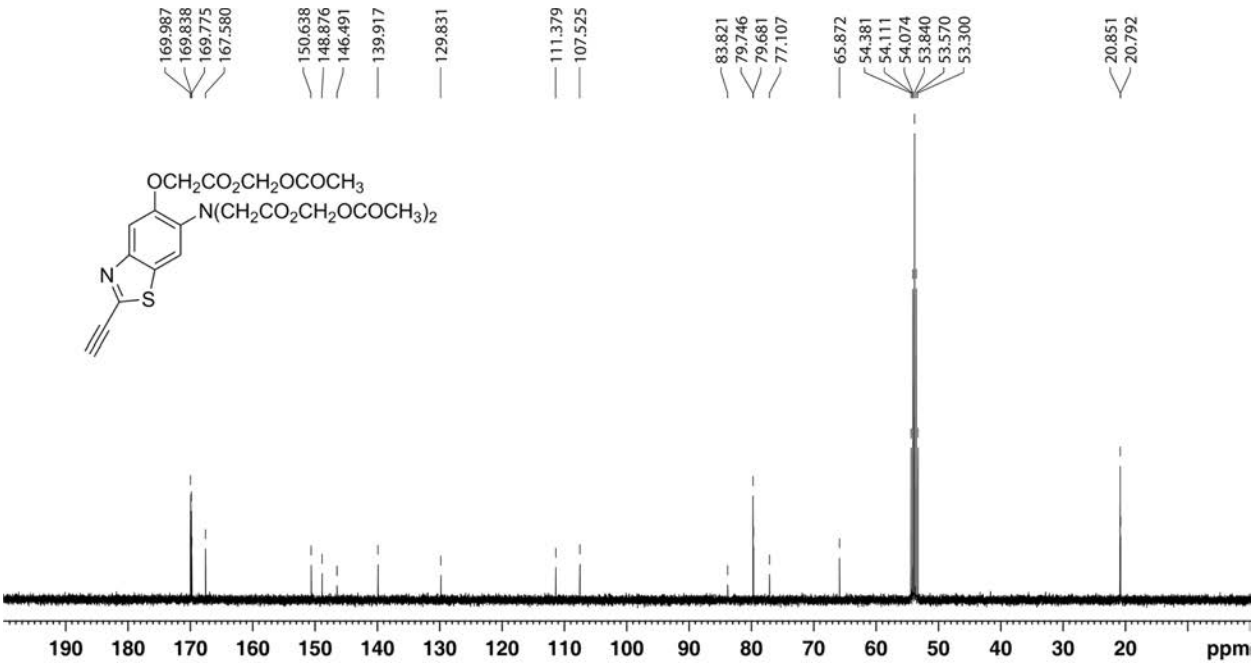

Figure S22. $^{13}C\{^{1}H\}$ NMR spectrum of compound **5-AM**, in CD_2Cl_2.

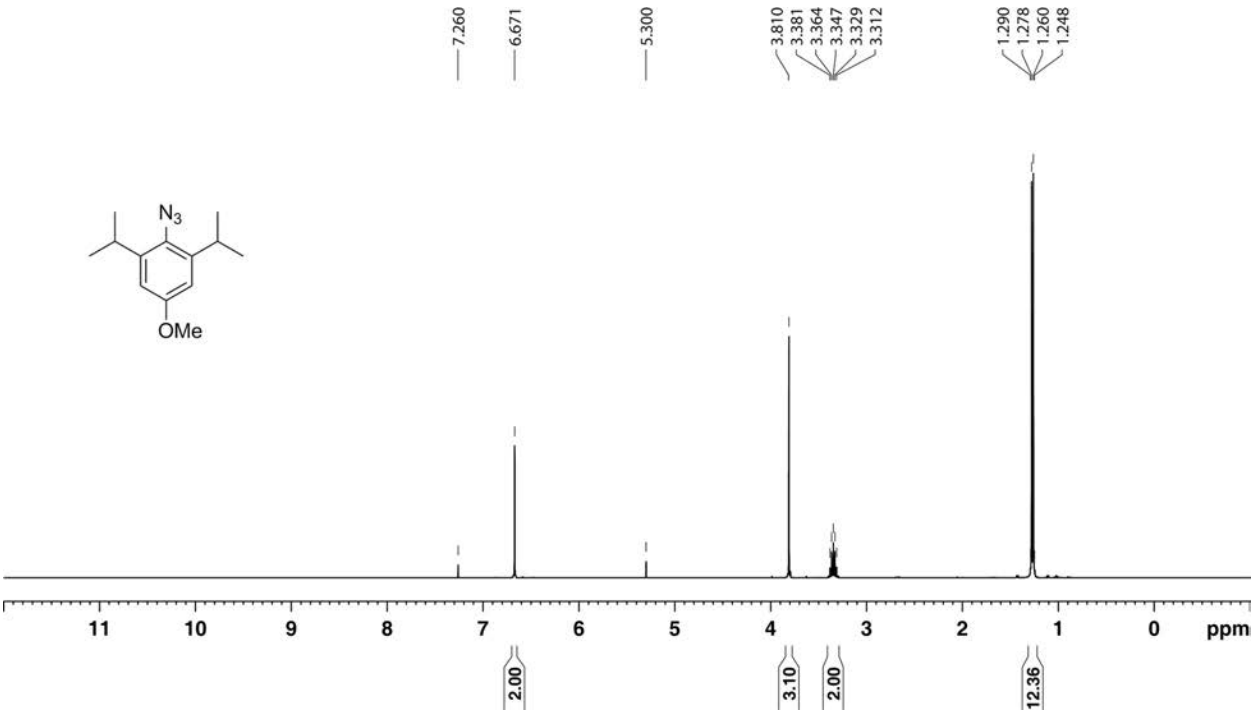

Figure S23. ^{1}H NMR spectrum of compound **8**, in $CDCl_3$.

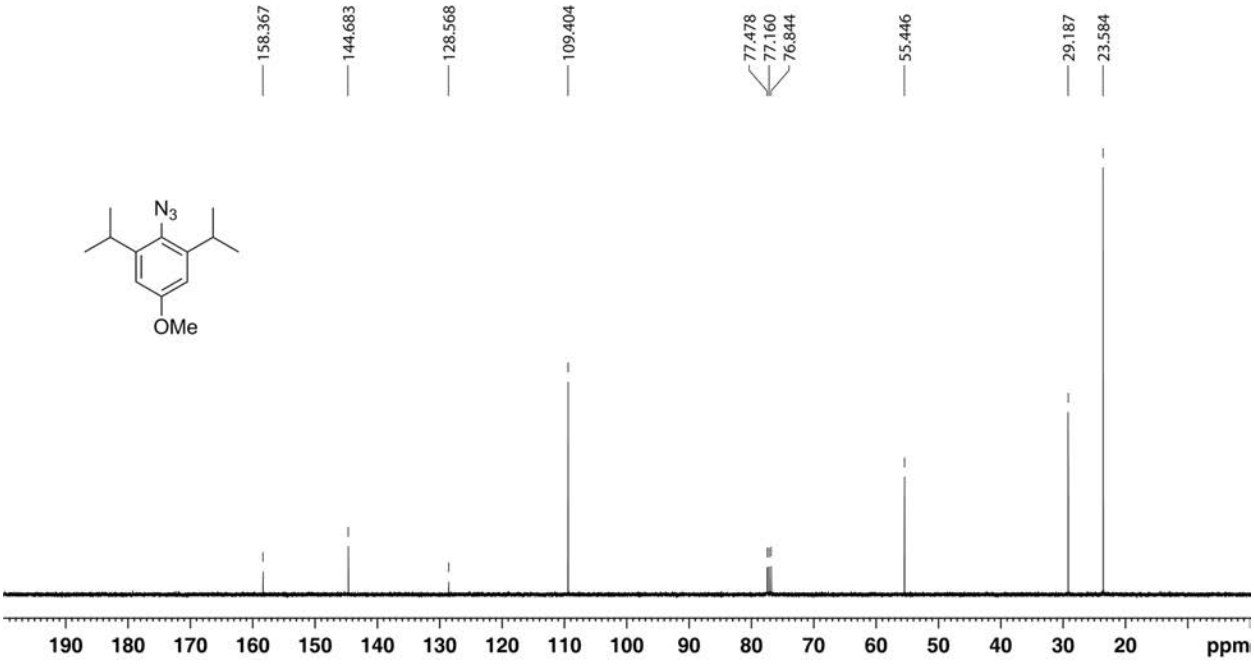

Figure S24. $^{13}C\{^{1}H\}$ NMR spectrum of compound **8**, in $CDCl_3$.

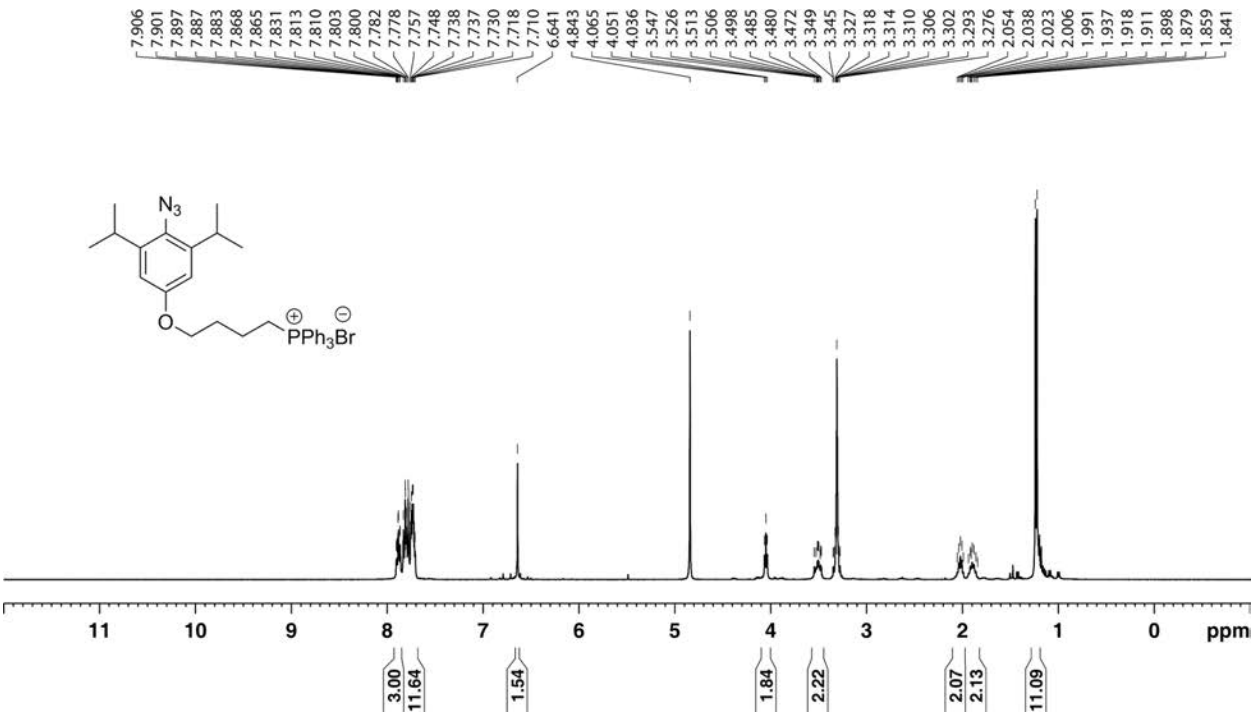

Figure S25. ^{1}H NMR spectrum of compound **13**, in CD_3OD.

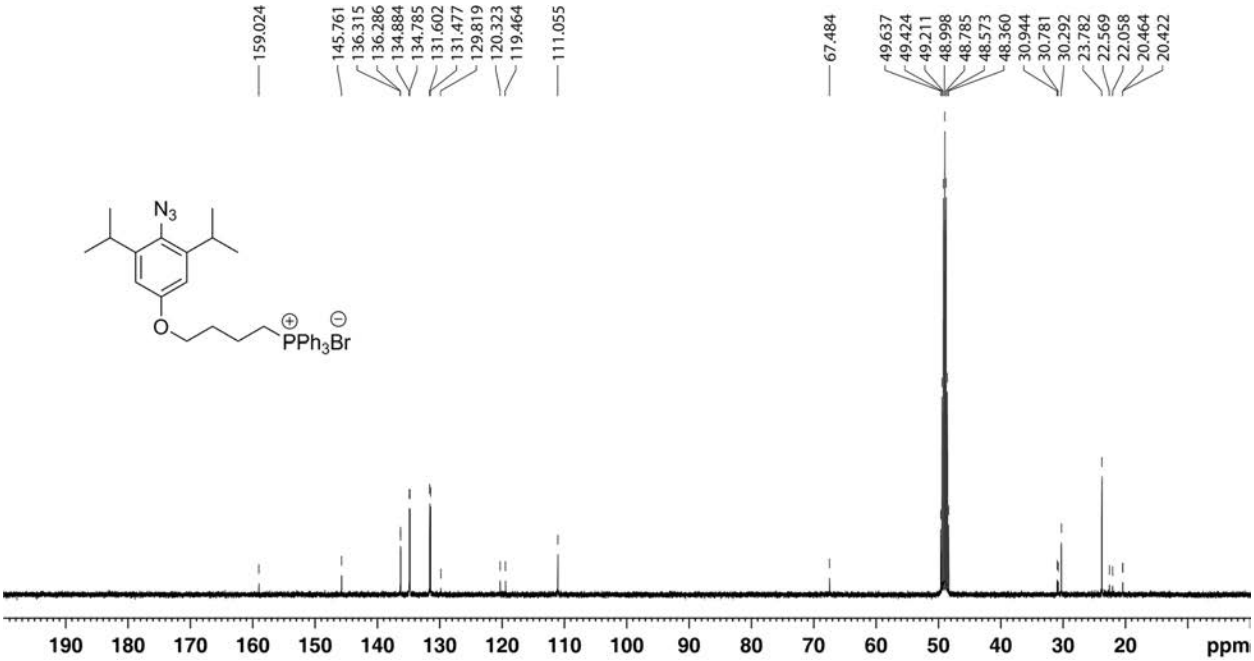

Figure S26. $^{13}C\{^{1}H\}$ NMR spectrum of compound **13**, in CD_3OD.

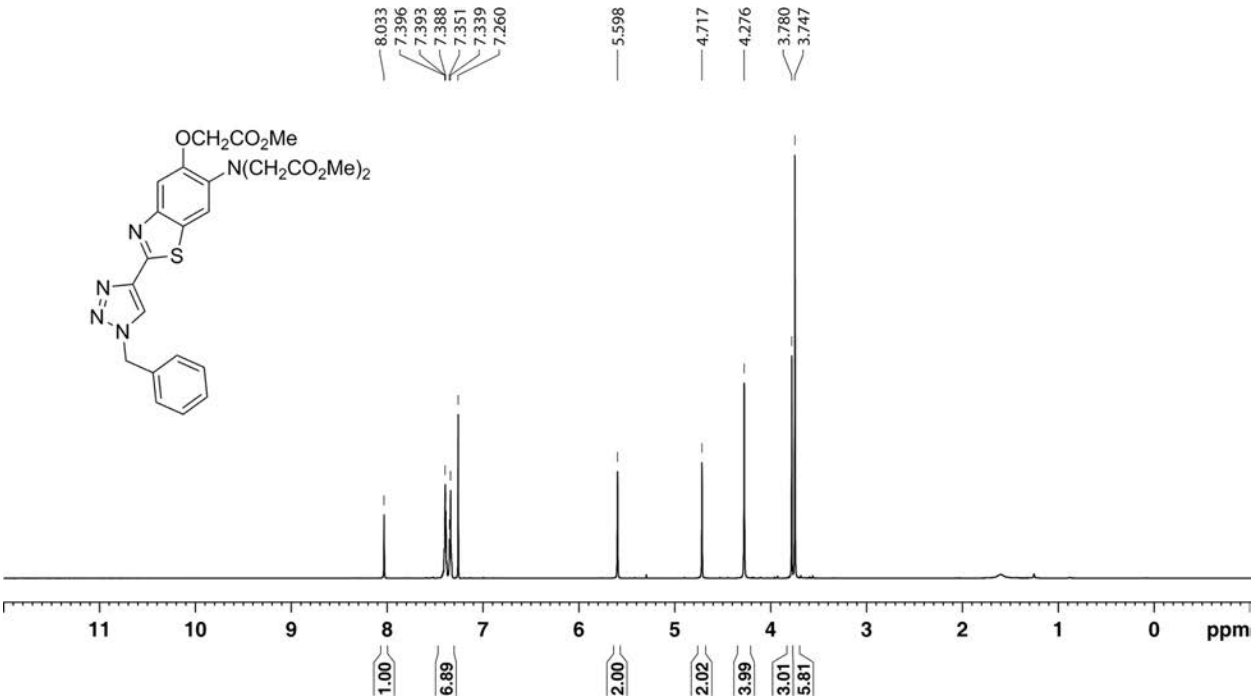

Figure S27. ^{1}H NMR spectrum of compound **6a**, in $CDCl_3$.

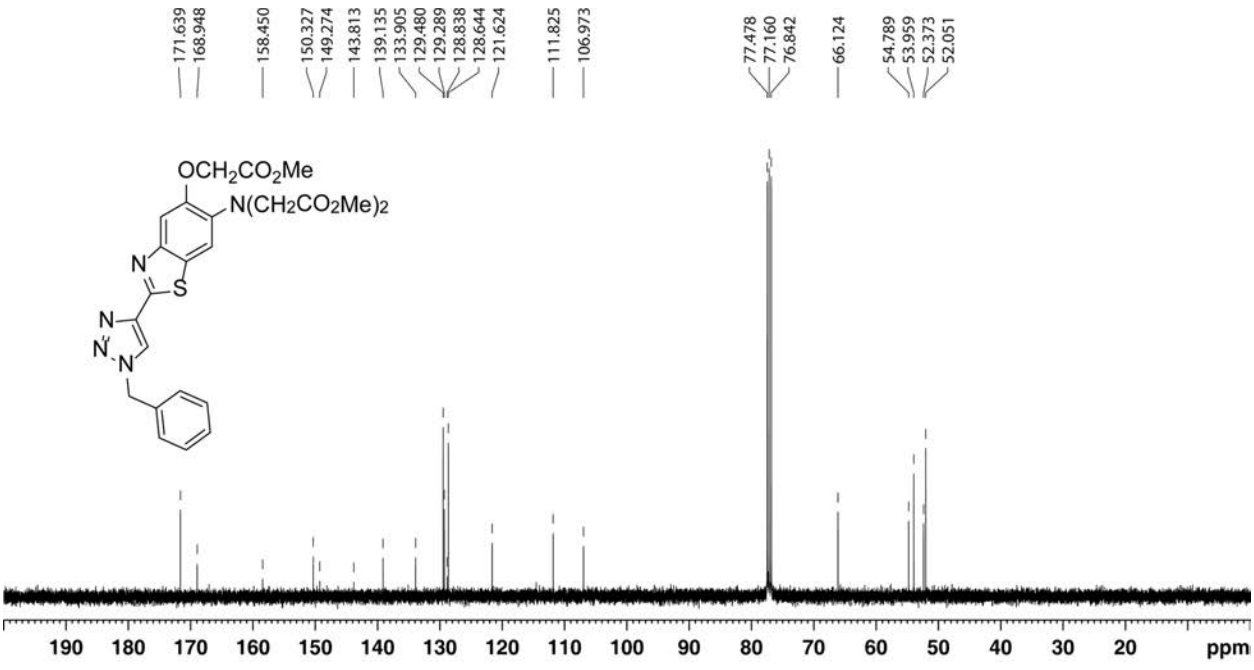

Figure S28. $^{13}C\{^{1}H\}$ NMR spectrum of compound **6a**, in $CDCl_3$.

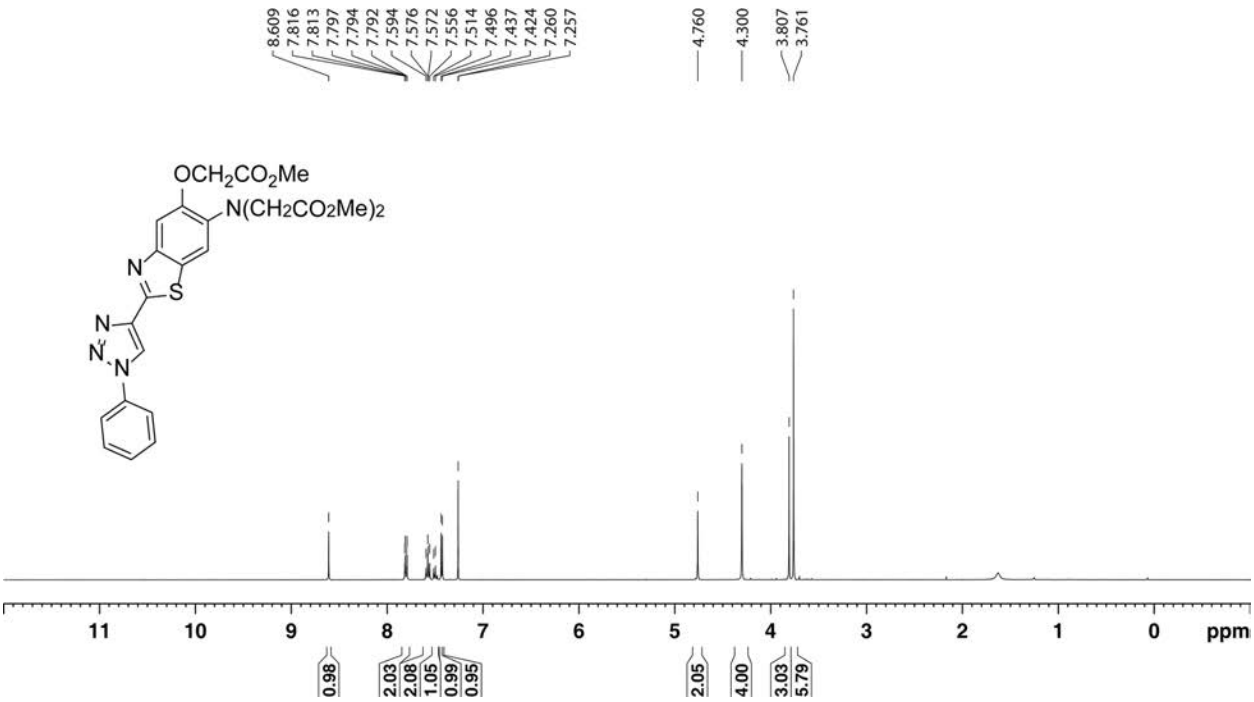

Figure S29. ^{1}H NMR spectrum of compound **6b**, in $CDCl_3$.

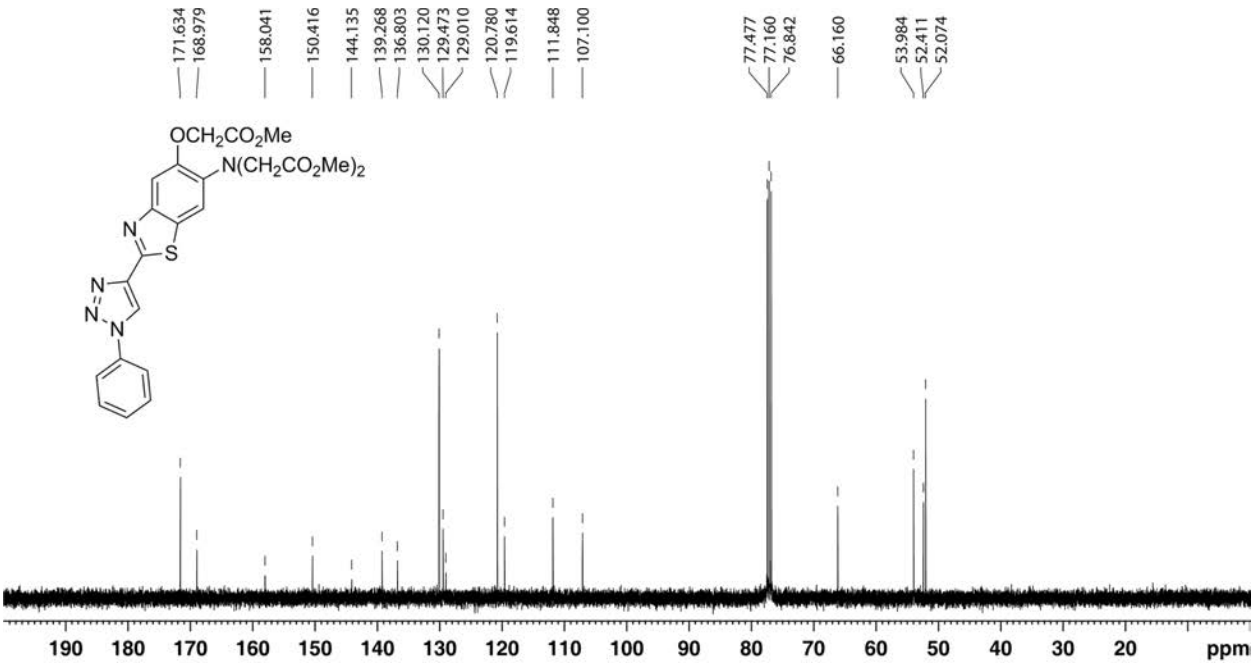

Figure S30. $^{13}C\{^{1}H\}$ NMR spectrum of compound **6b**, in $CDCl_3$.

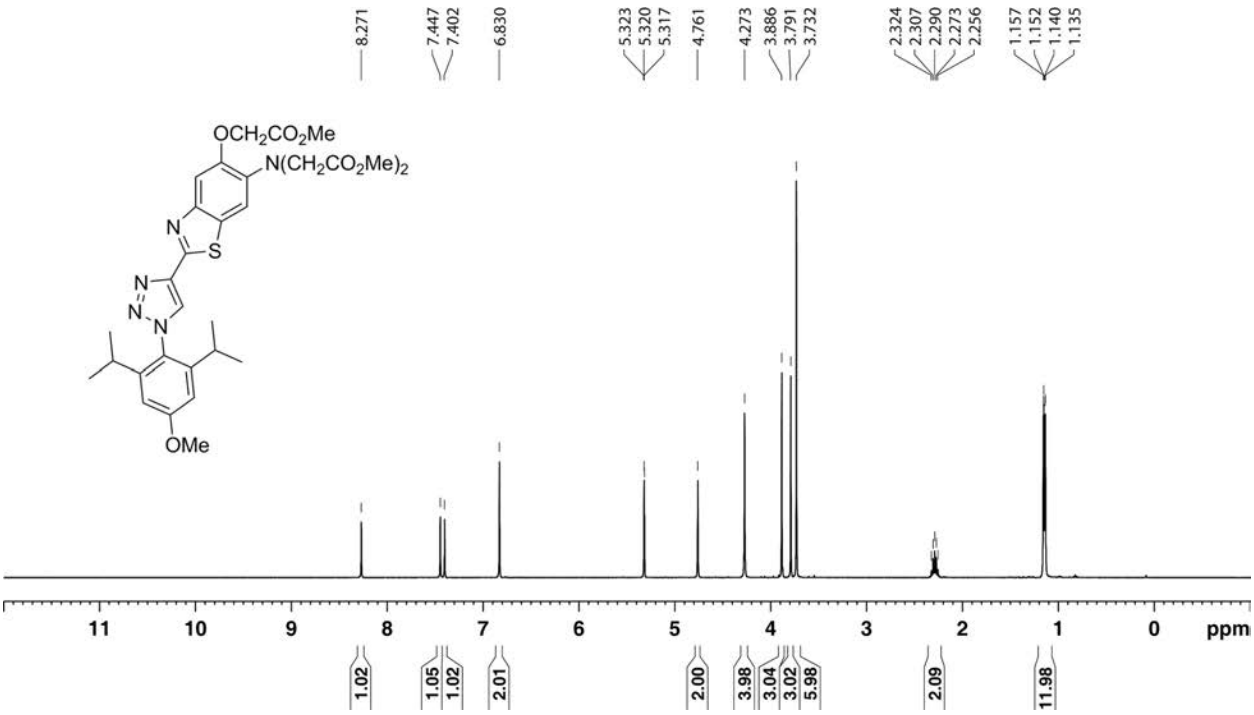

Figure S31. ^{1}H NMR spectrum of compound **6c**, in CD_2Cl_2.

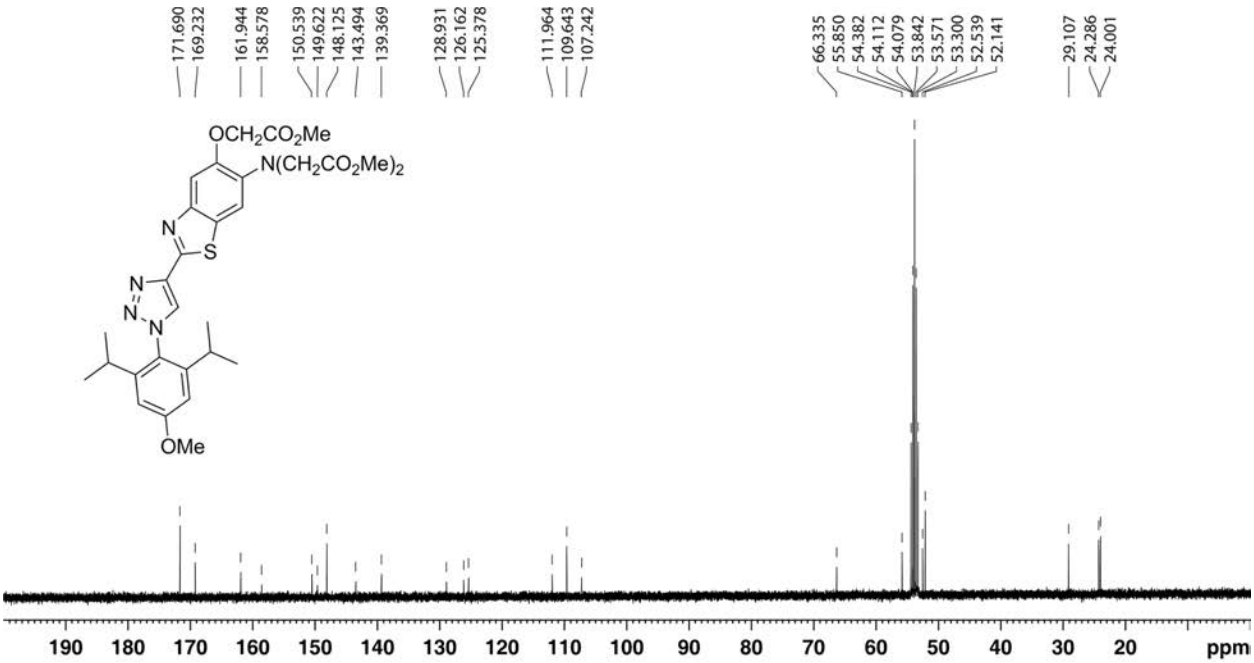

Figure S32. $^{13}C\{^{1}H\}$ NMR spectrum of compound **6c**, in CD_2Cl_2.

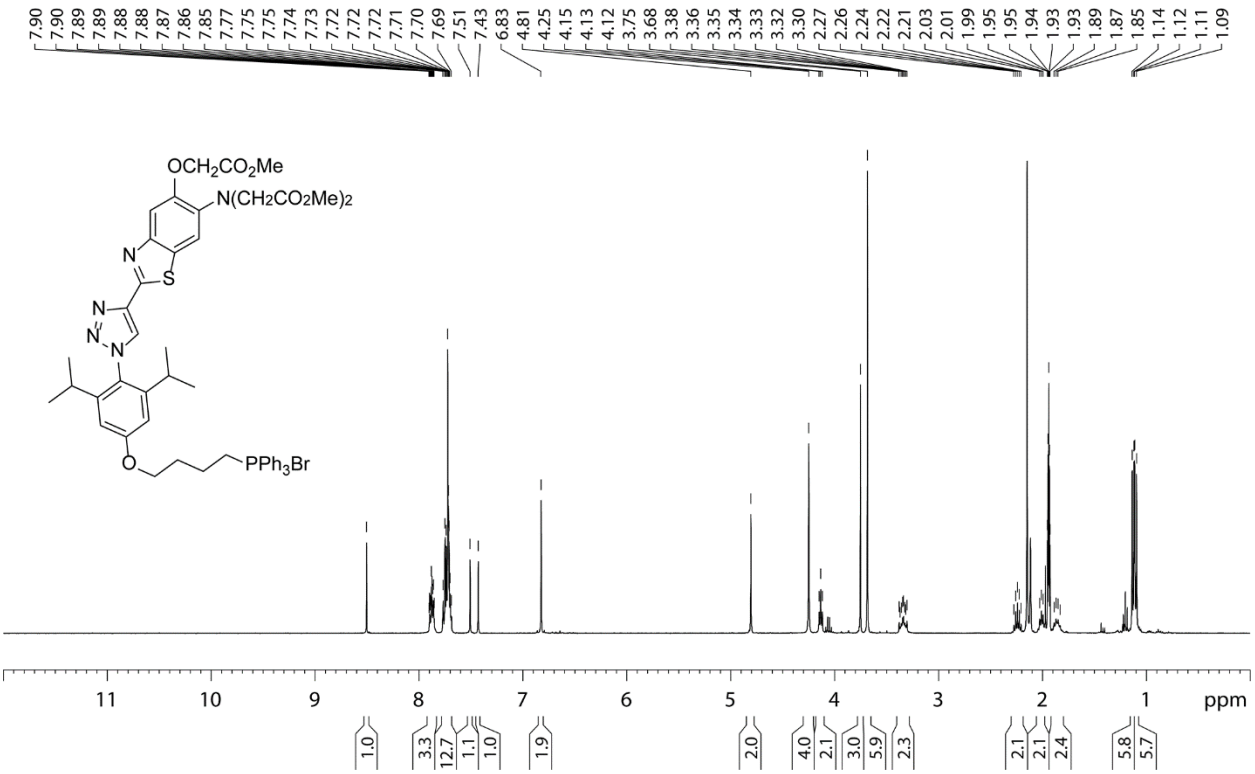

Figure S33. ^{1}H NMR spectrum of compound **6d**, in CD_3CN.

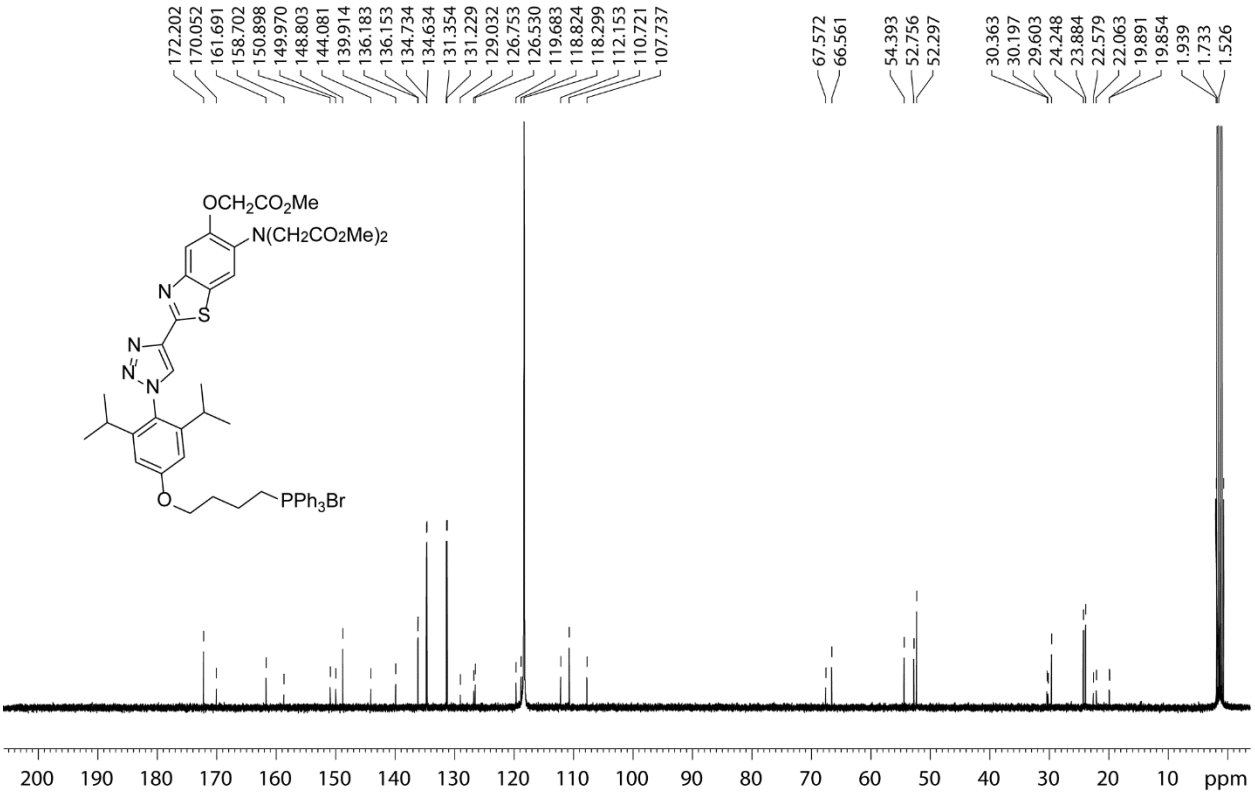

Figure S34. $^{13}C\{^{1}H\}$ NMR spectrum of compound **6d**, in CD_3CN.

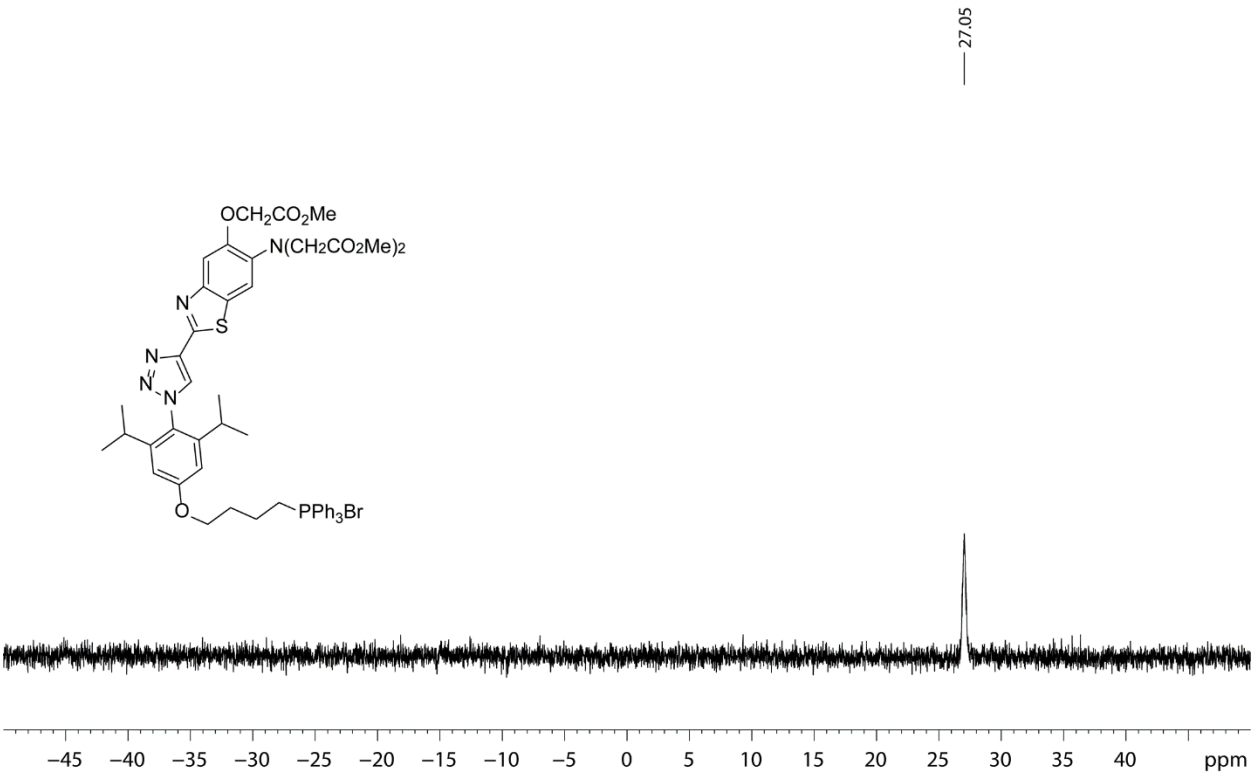

Figure S35. ^{31}P NMR spectrum of compound **6d**, in CD_3CN.

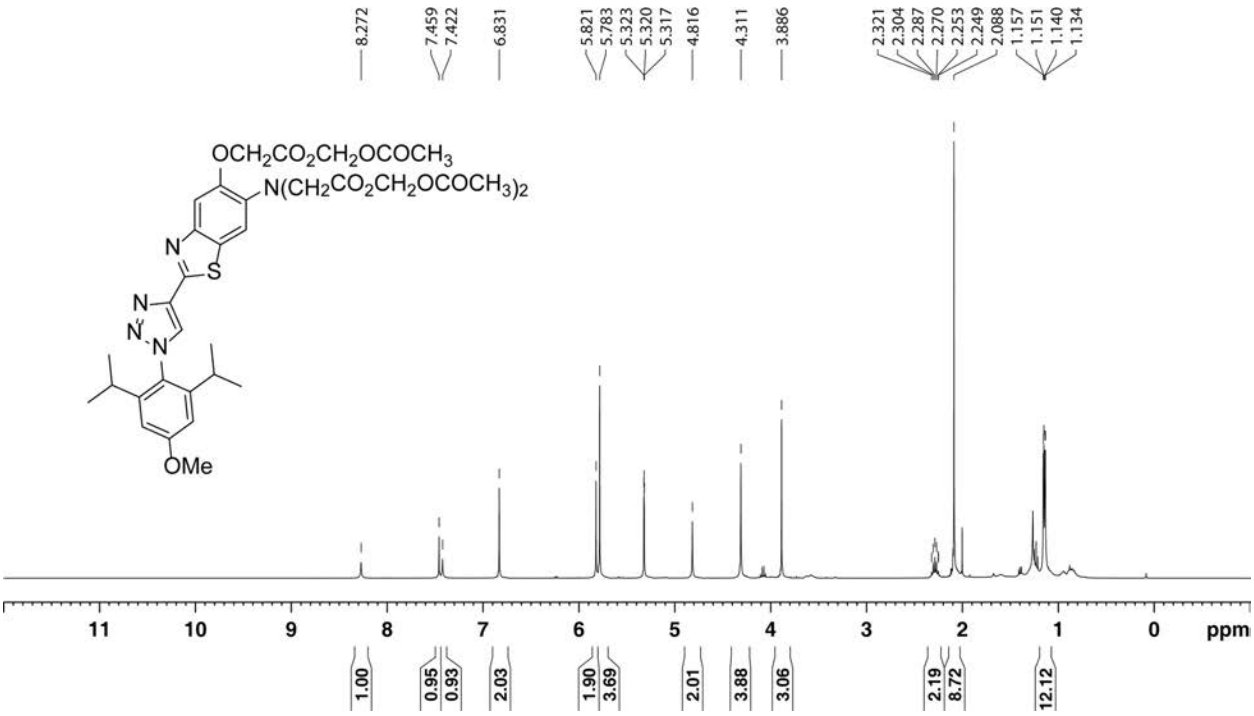

Figure S36. ^{1}H NMR spectrum of compound **7c-AM**, in CD_2Cl_2.

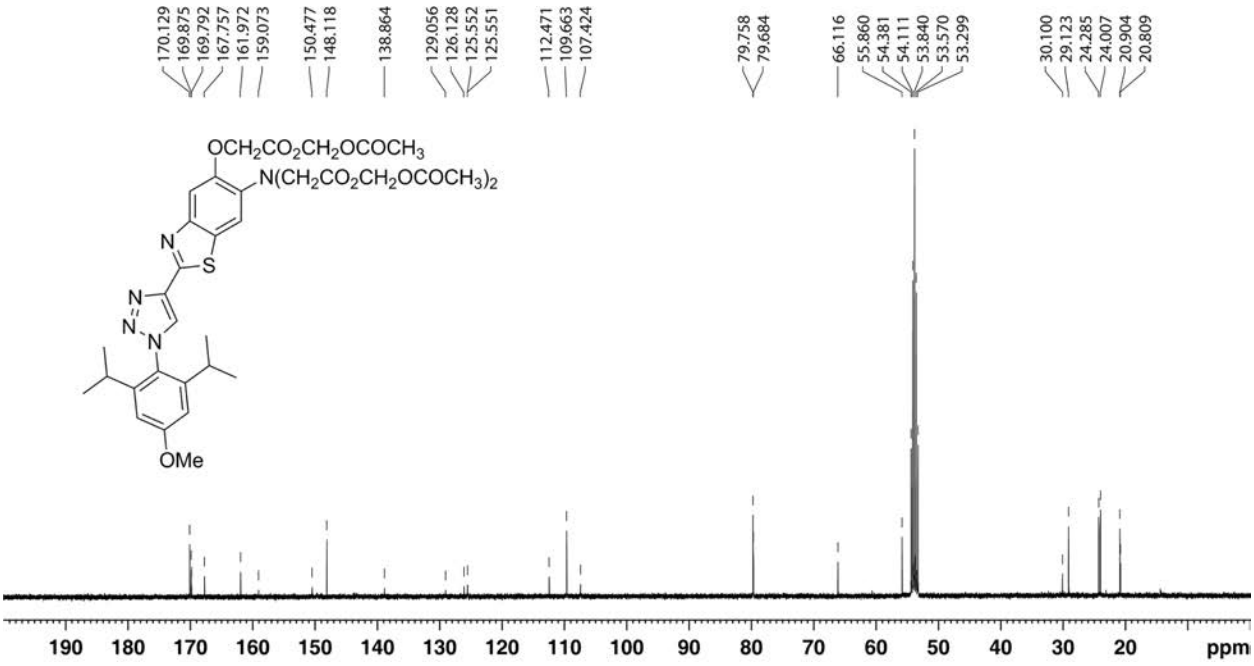

Figure S37. $^{13}C\{^{1}H\}$ NMR spectrum of compound **7c-AM**, in CD_2Cl_2.

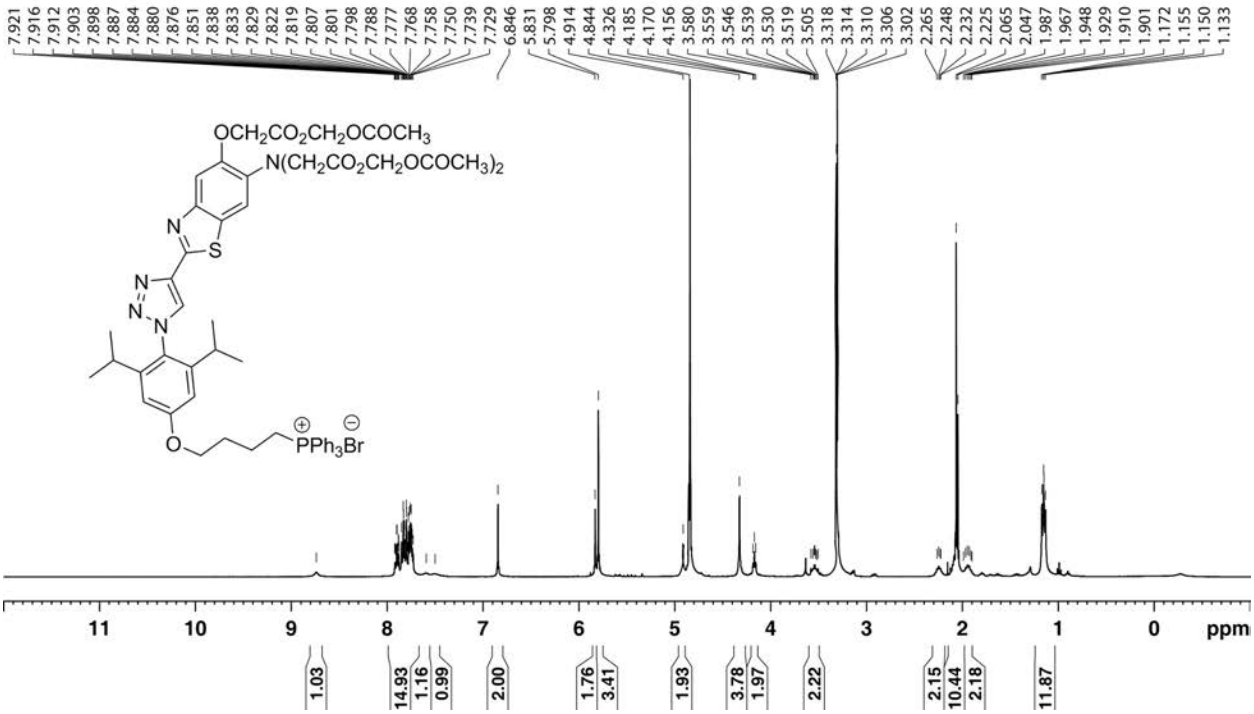

Figure S38. ^{1}H NMR spectrum of compound **Mag-*mito*-AM**, in CD_3OD.

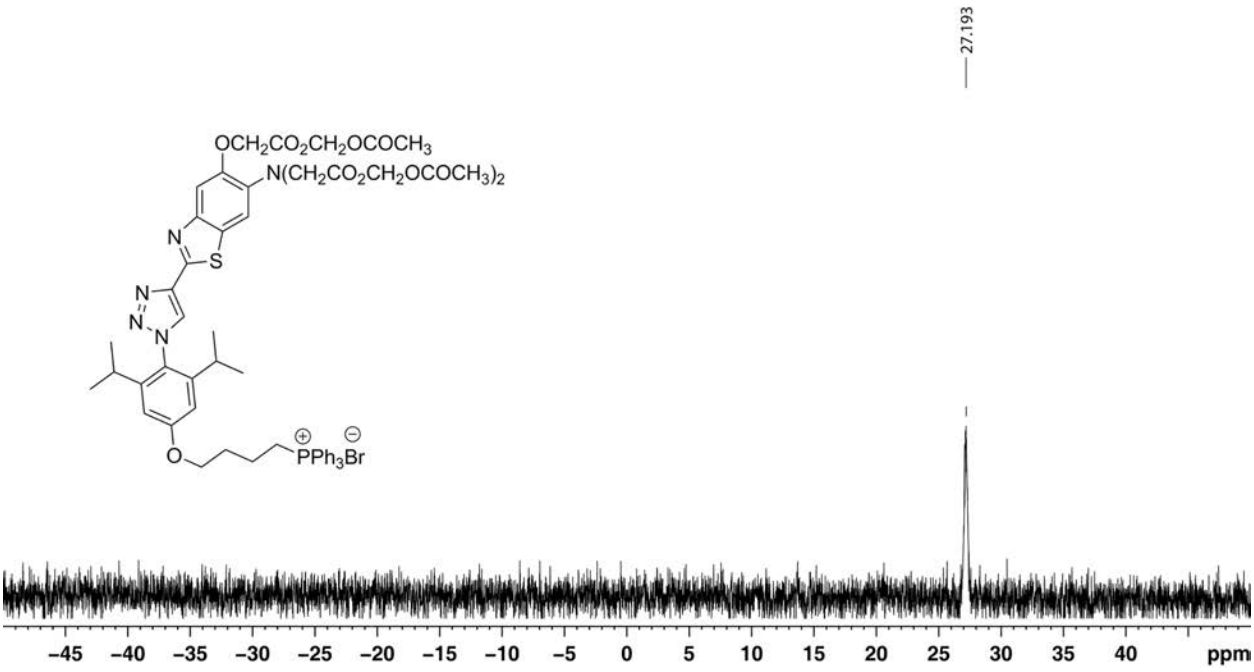

Figure S39. ^{31}P NMR spectrum of compound **Mag-*mito*-AM**, in CD_3OD.

6. HPLC data for new sensors

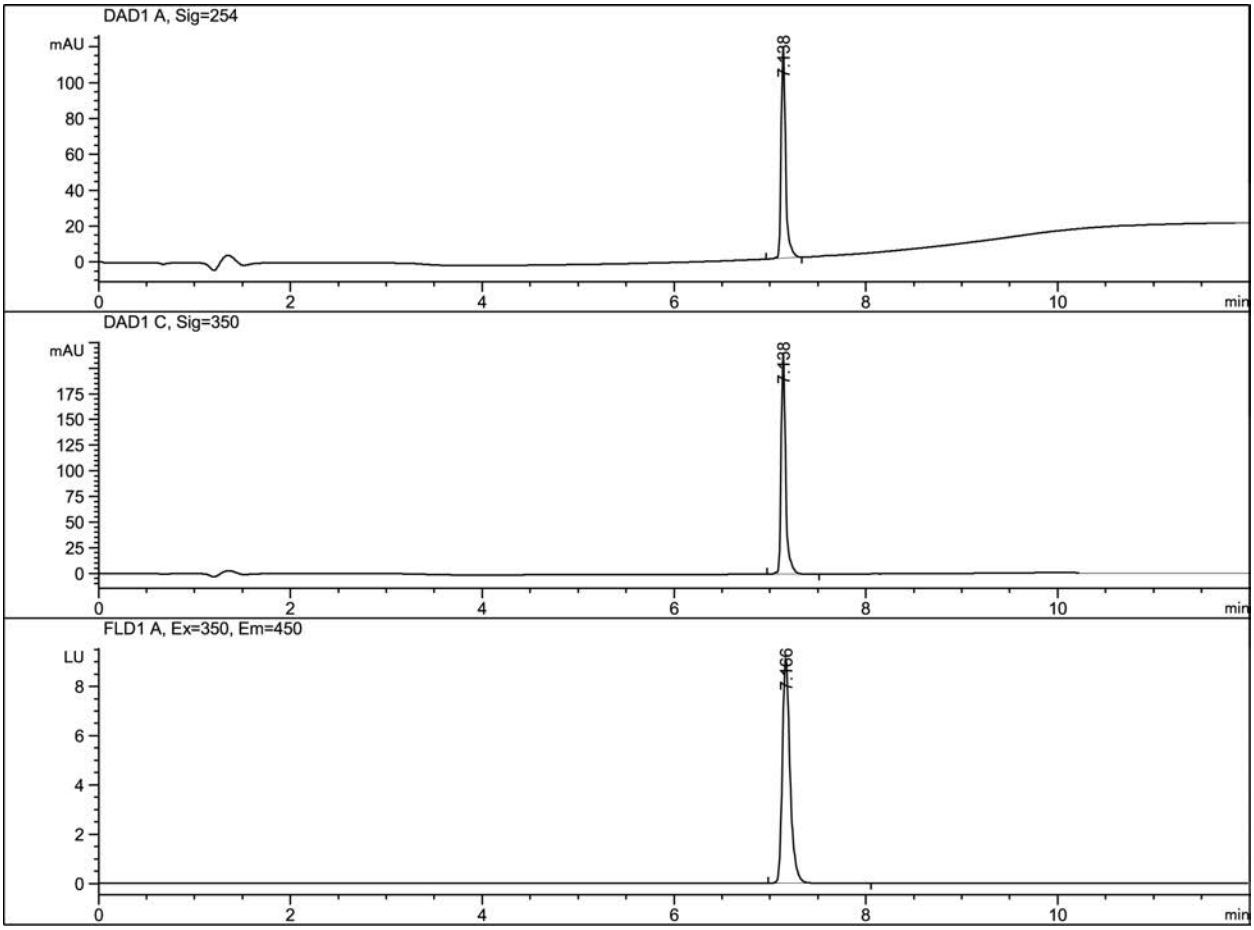

Figure S40. Reversed phase HPLC chromatogram of compound **6a**, eluted with an acetonitrile/water (+0.1% TFA) gradient.

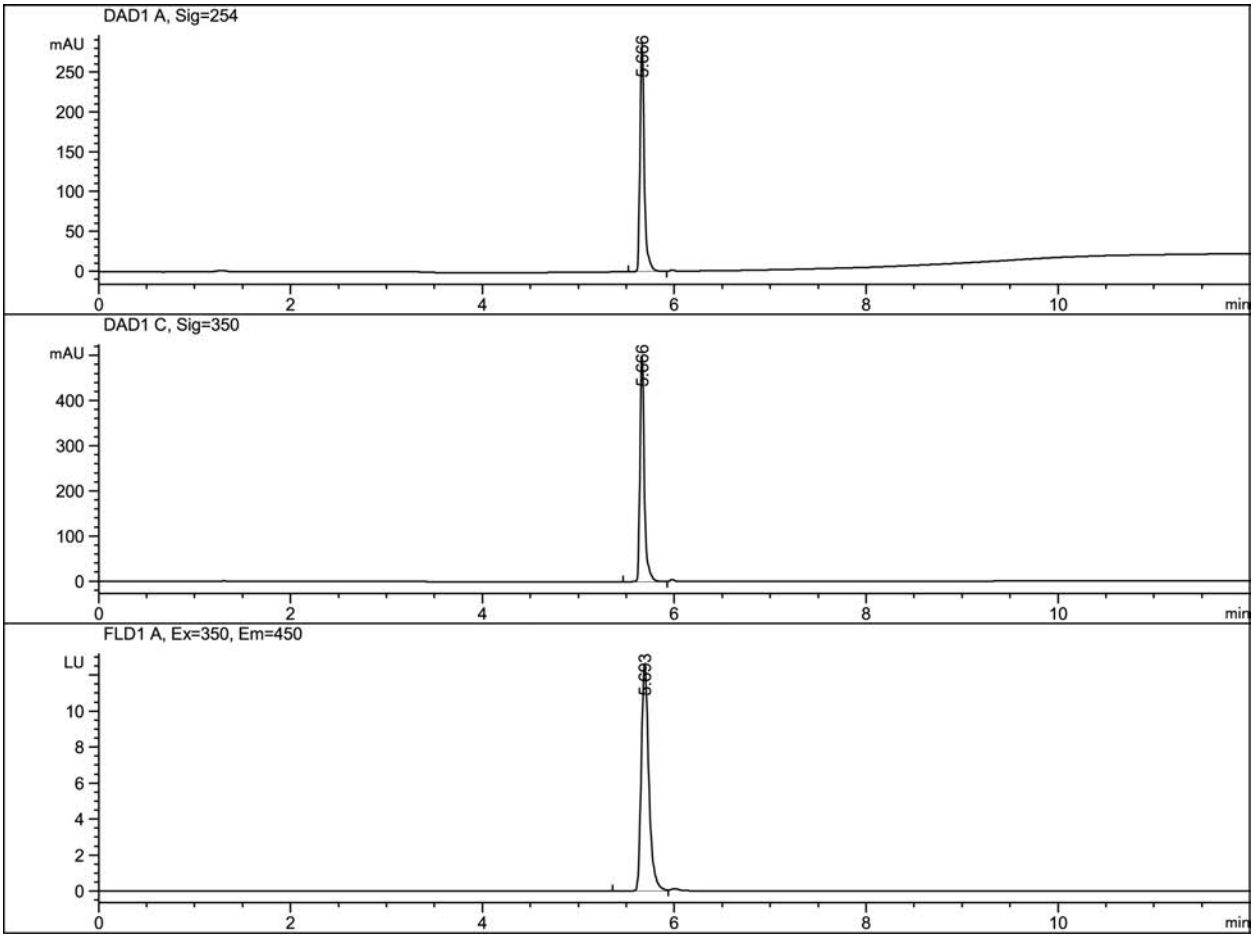

Figure S41. Reversed phase HPLC chromatogram of compound **7a**, eluted with an acetonitrile/water (+0.1% TFA) gradient.

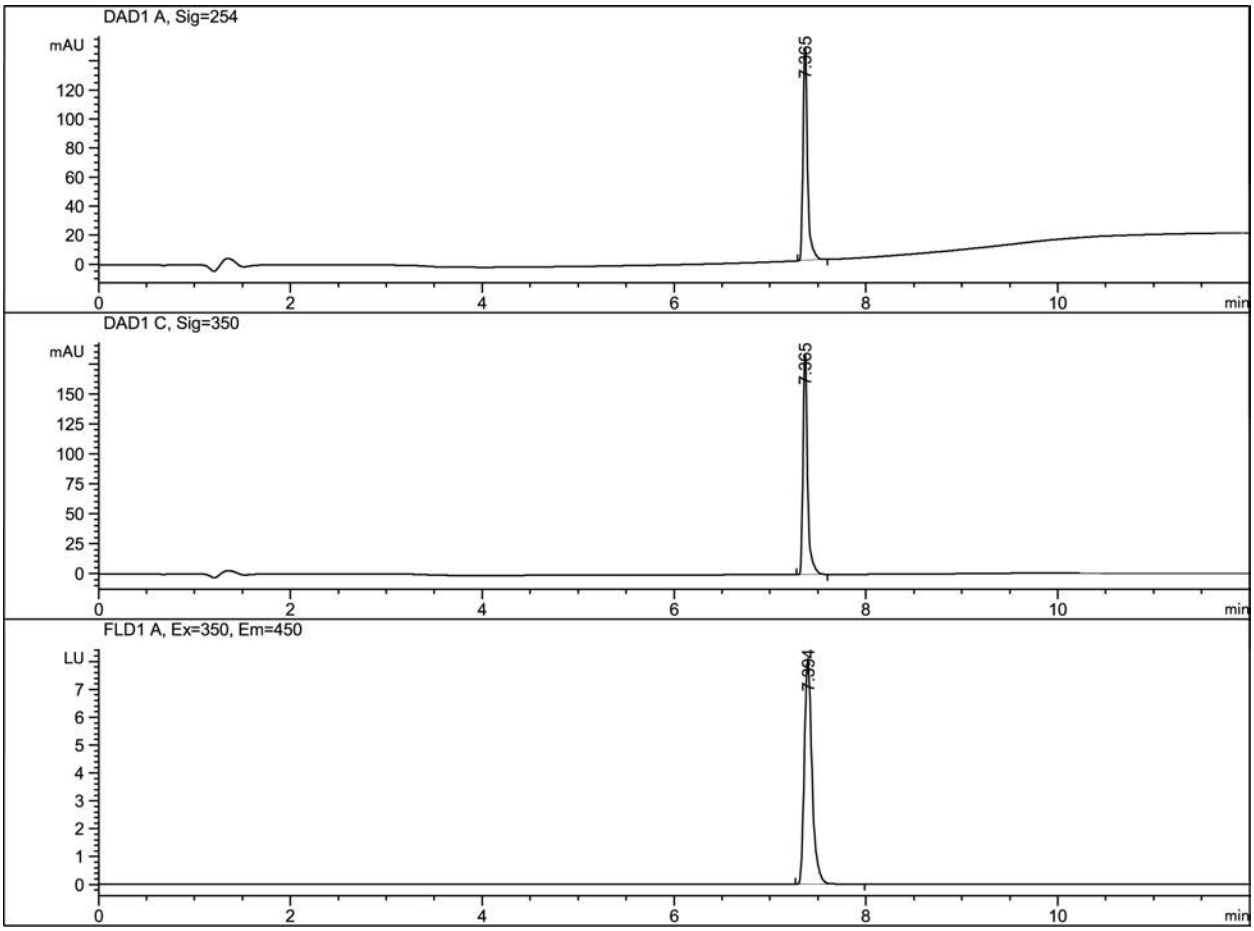

Figure S42. Reversed phase HPLC chromatogram of compound **6b**, eluted with an acetonitrile/water (+0.1% TFA) gradient.

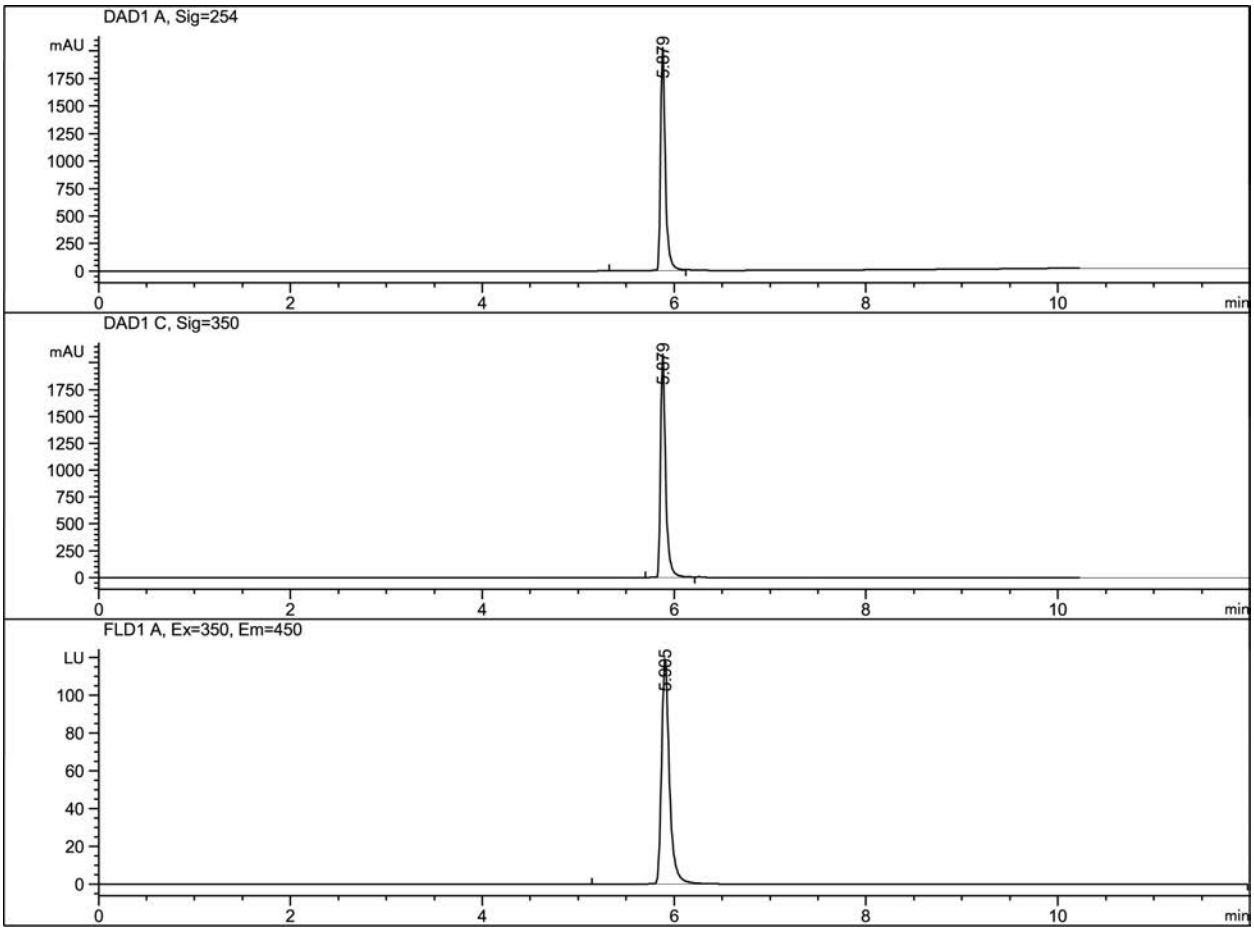

Figure S43. Reversed phase HPLC chromatogram of compound **7b**, eluted with an acetonitrile/water (+0.1% TFA) gradient.

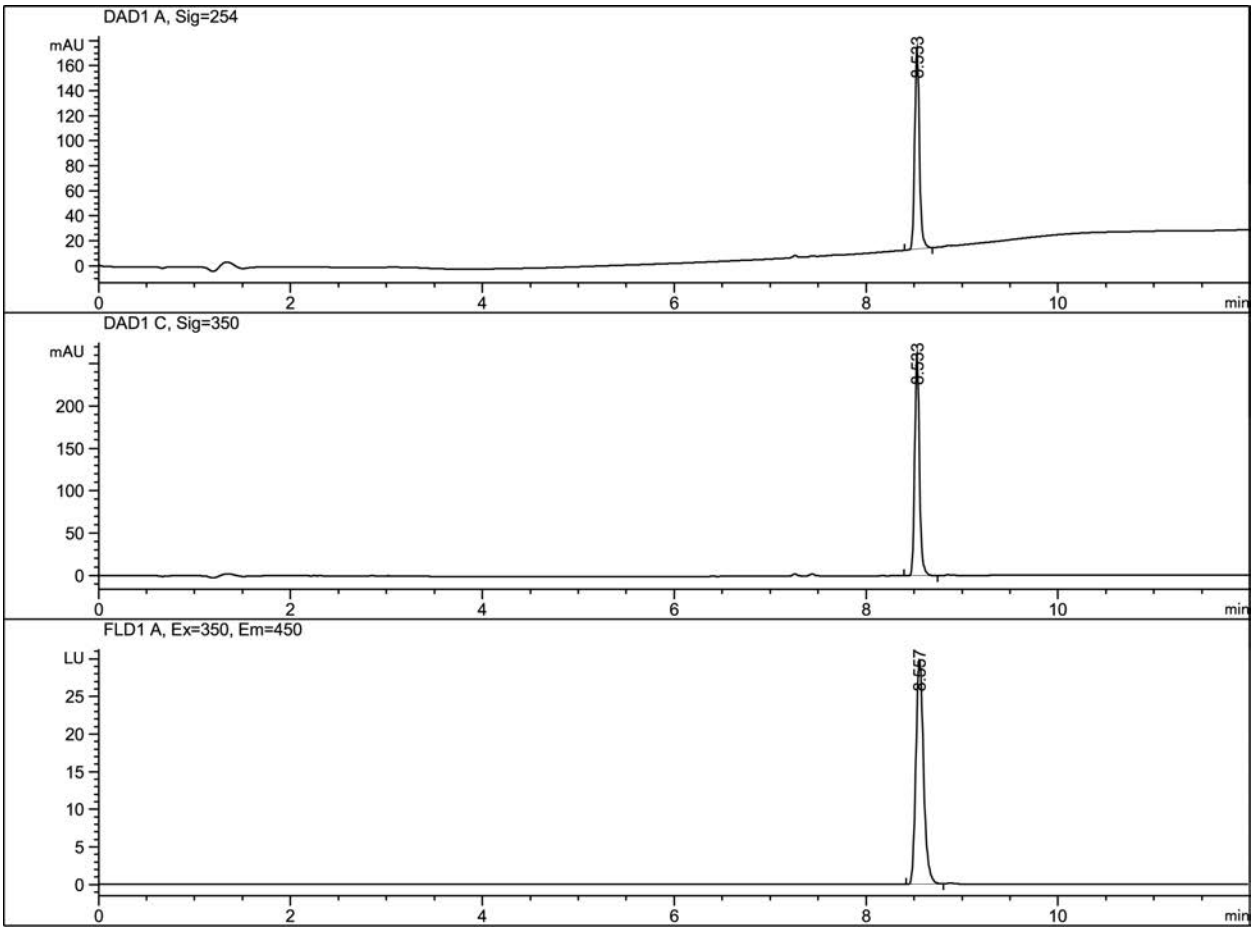

Figure S44. Reversed phase HPLC chromatogram of compound **6c**, eluted with an acetonitrile/water (+0.1% TFA) gradient.

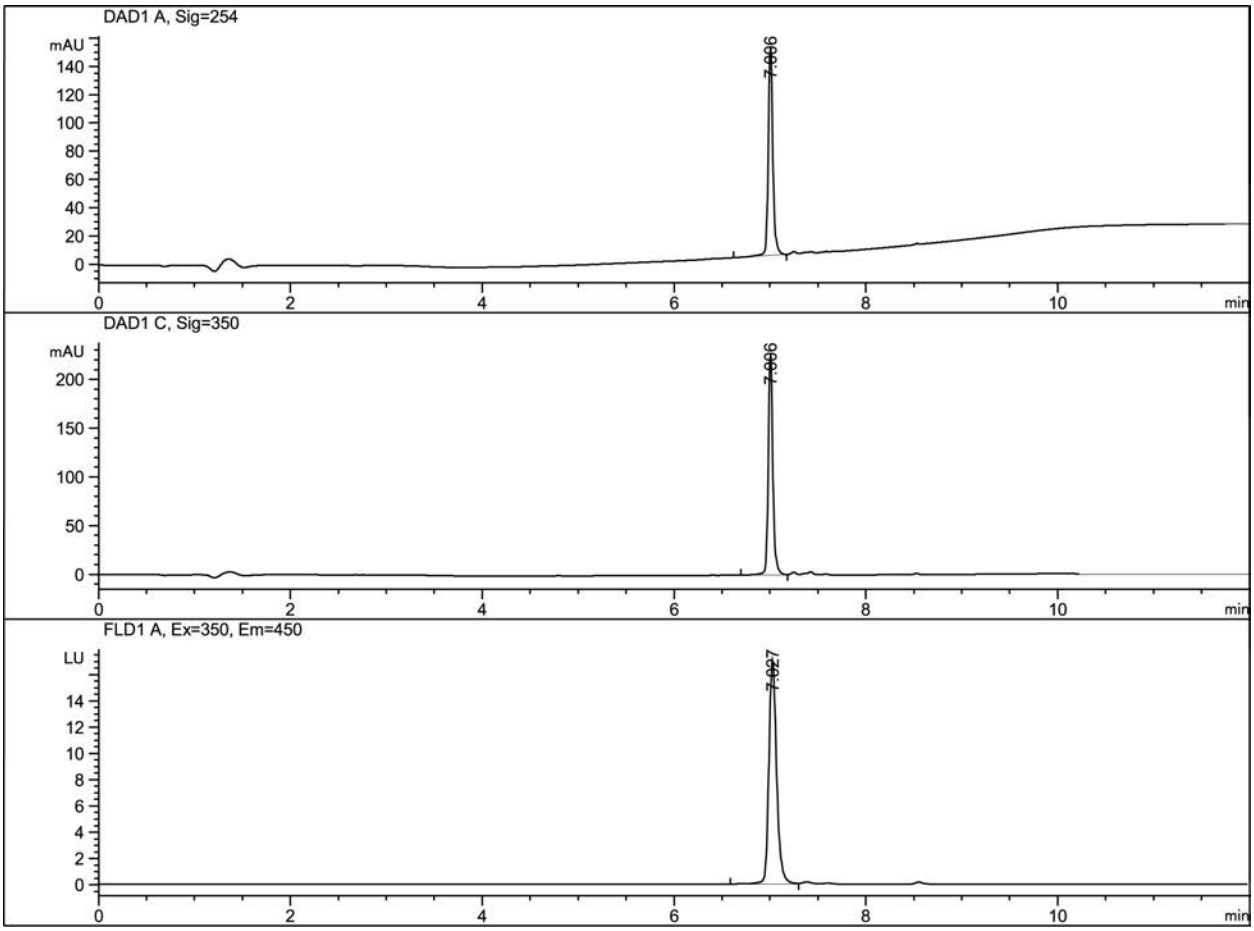

Figure S45. Reversed phase HPLC chromatogram of compound **7c**, eluted with an acetonitrile/water (+0.1% TFA) gradient.

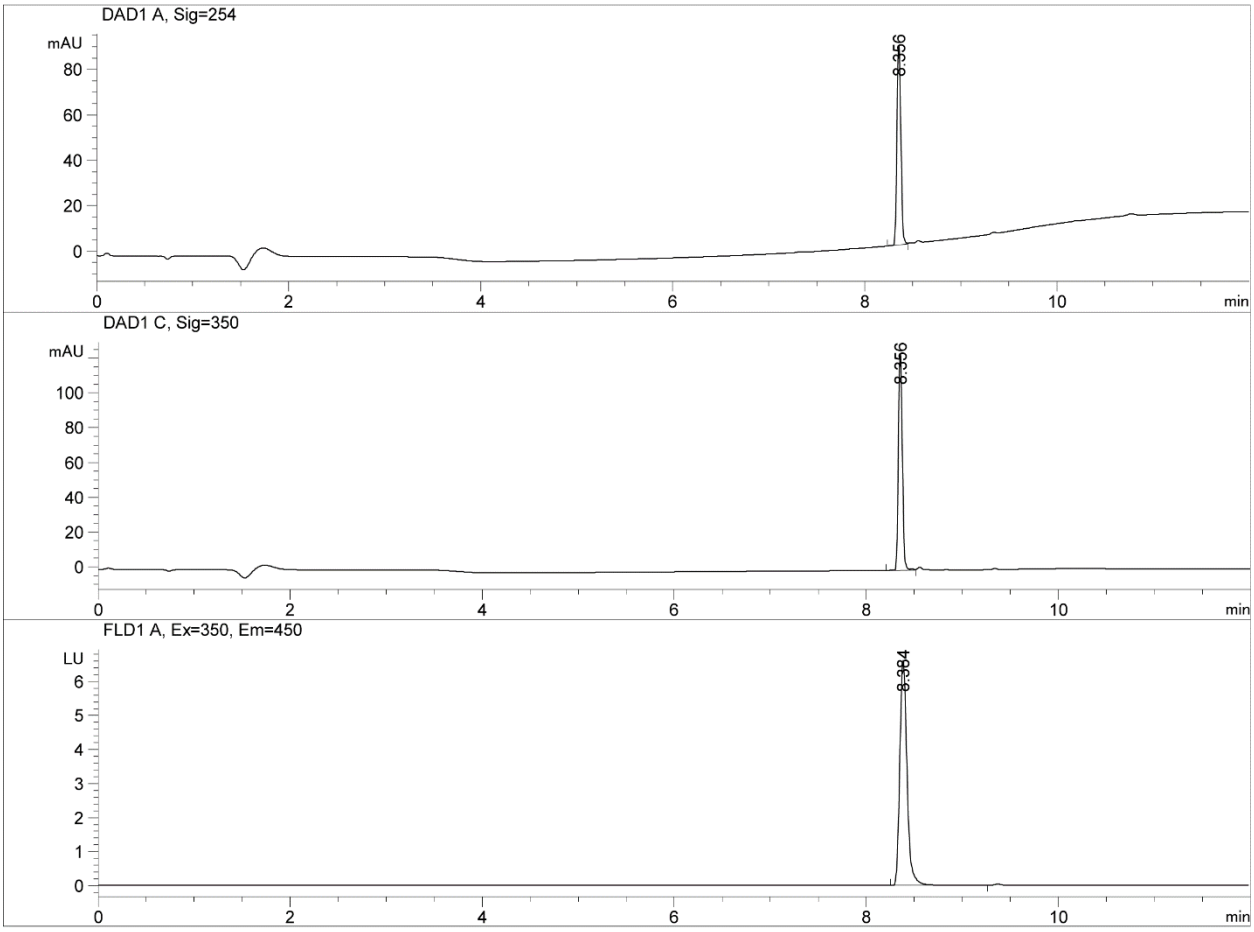

Figure S46. Reverse phase HPLC chromatogram of compound **6d** eluted with an acetonitrile/water (+0.1% TFA) gradient.

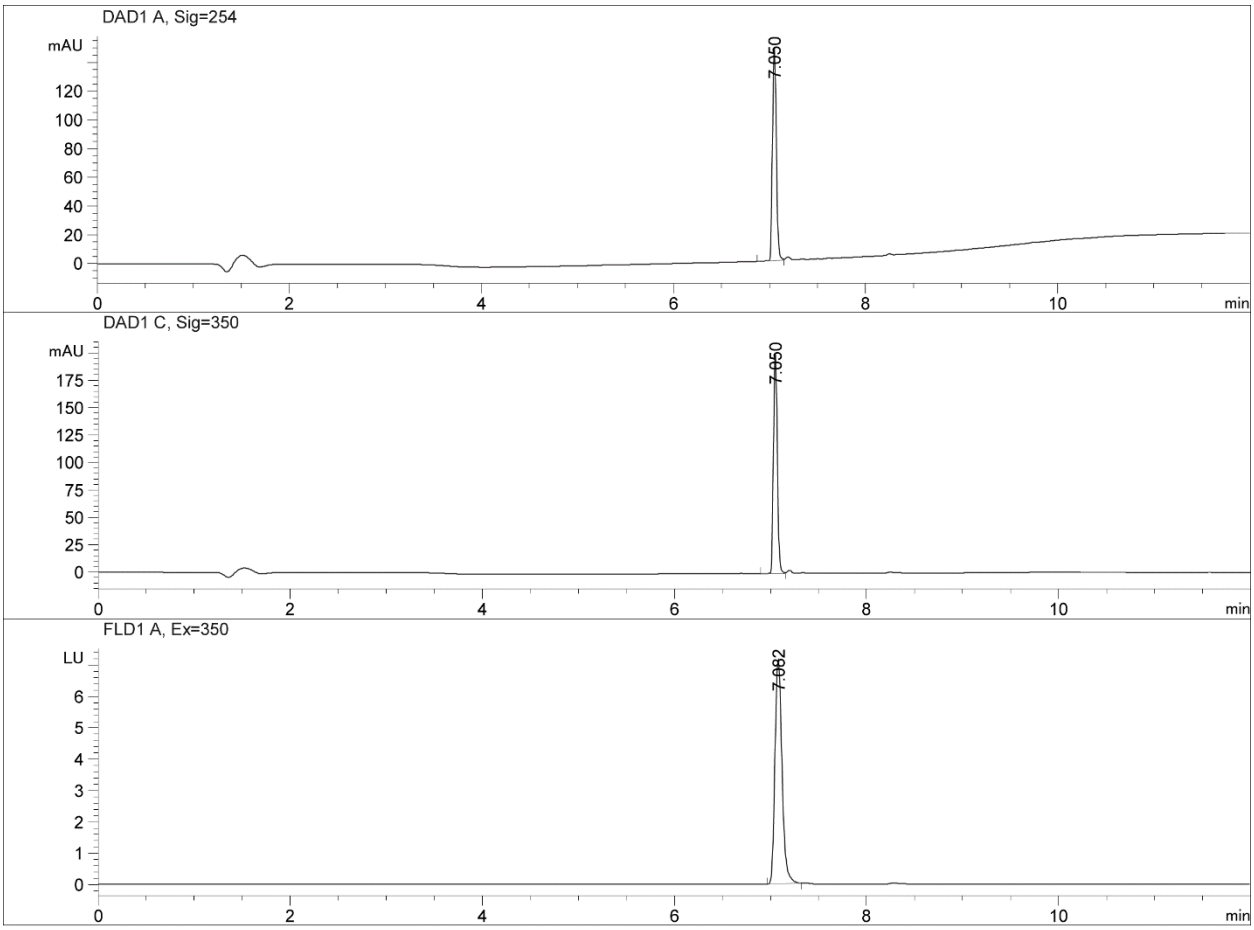

Figure S47. Reverse phase HPLC chromatogram of **Mag-*mito***, free acid, eluted with an acetonitrile/water (+0.1% TFA) gradient.

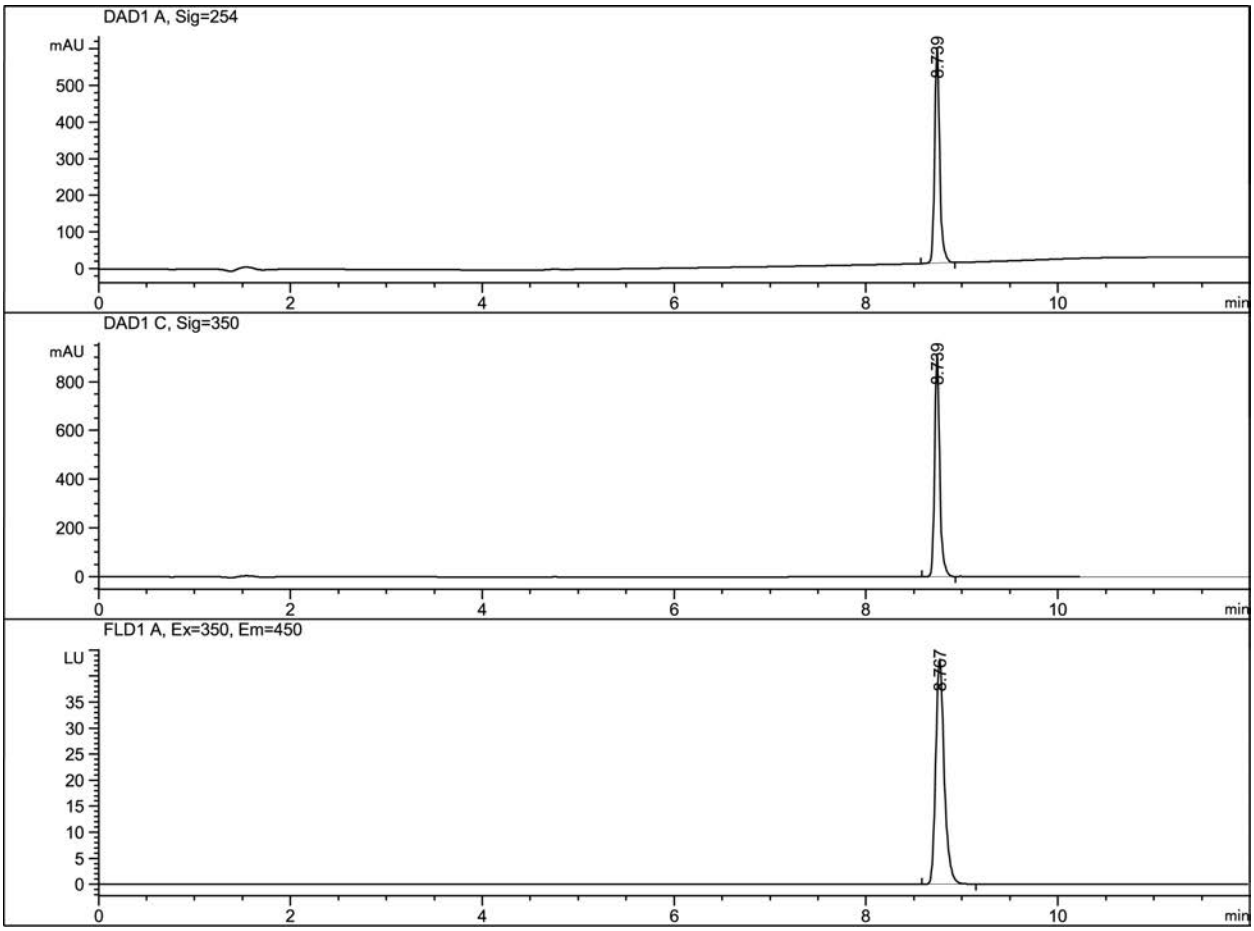

Figure S48. Reversed phase HPLC chromatogram of compound **7c-AM**, eluted with an acetonitrile/water (+0.1% TFA) gradient.

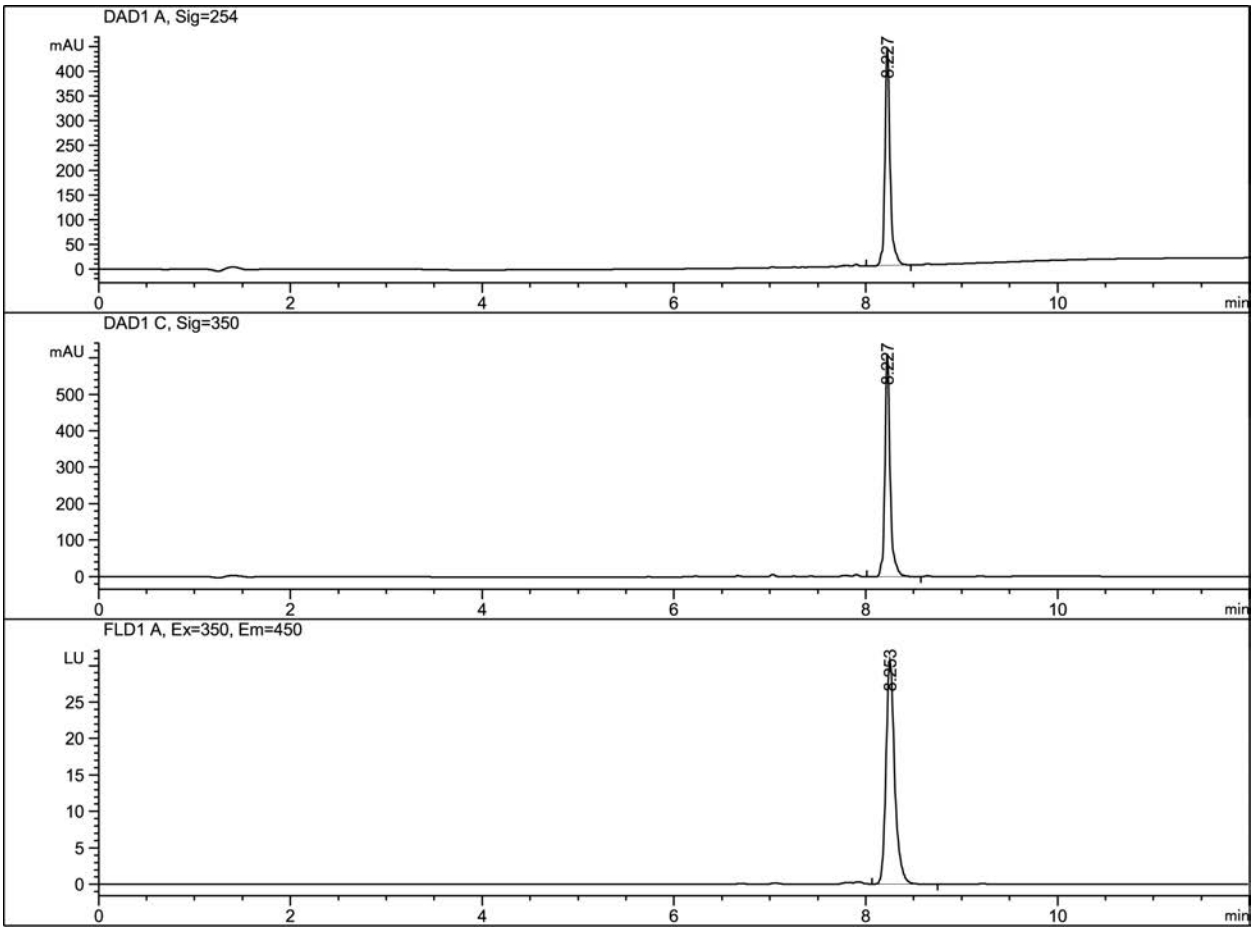

Figure S49. Reversed phase HPLC chromatogram of compound **Mag-*mito*-AM**, eluted with an acetonitrile/water (+0.1% TFA) gradient.

7. References

[1] R. K. Gupta, P. Gupta, W. D. Yushok, Z. B. Rose, *Biochem. Biophys. Res. Commun.* **1983**, *117*, 210-216.

[2] B. Metten, M. Smet, N. Boens, W. Dehaen, *Synthesis* **2005**, *2005*, 1838-1844.

[3] T. K. Lane, B. R. D'Souza, J. Louie, *J. Org. Chem.* **2012**, *77*, 7555-7563.

[4] A. Hospital, C. Gibard, C. Gaulier, L. Nauton, V. Thery, M. El-Ghozzi, D. Avignant, F. Cisnetti, A. Gautier, *Dalton Trans.* **2012**, *41*, 6803-6812.

[5] A. M. Brouwer, *Pure Appl. Chem.* **2011**, *83*, 2213-2228.

[6] G. Grynkiewicz, M. Poenie, R. Y. Tsien, *J. Biol. Chem.* **1985**, *260*, 3440-3450.

[7] A. E. Hargrove, Z. Zhong, J. L. Sessler, E. V. Anslyn, *New J. Chem.* **2010**, *34*, 348-354.

[8] A. E. Palmer, M. Giacomello, T. Kortemme, S. A. Hires, V. Lev-Ram, D. Baker, R. Y. Tsien, *Chem. Biol.* **2006**, *13*, 521-530.

[9] V. Trapani, M. Schweigel-Rontgen, A. Cittadini, F. I. Wolf, in *Methods Enzymol., Vol. 505* (Ed.: P. M. Conn), Academic Press, **2012**, pp. 421-444.

[10] A. E. Palmer, R. Y. Tsien, *Nat. Protocols* **2006**, *1*, 1057-1065.